L

LAKE ELLSWORTH

John Woodward[1], Martin J. Siegert[2], Andy M. Smith[3], Neil Ross[4]
[1]Division of Geography, School of Applied Sciences, Northumbria University, Newcastle upon Tyne, UK
[2]School of GeoSciences, University of Edinburgh, Grant Institute, Edinburgh, UK
[3]British Antarctic Survey, High Cross, Cambridge, UK
[4]School of Geosciences, University of Edinburgh, Geography Building, Edinburgh, UK

Introduction

Subglacial Lake Ellsworth is located near the Ellsworth Mountains in West Antarctica at 78.9°S 90.6°W. The lake basin is in the center of the West Antarctic Ice Sheet (WAIS) in the Pine Island Glacier drainage basin, 20 km from the ice divide with the Institute Ice Stream. The lake is approximately 15 km long and over 3 km across at its widest point. Seismic surveys have revealed that the lake is over 100 m deep in places. The ice sheet above the lake is between 2.9 and 3.3 km thick, with the lake surface over 1 km beneath present sea level within a distinct topographic hollow, ~1.5 km deeper than the surrounding subglacial bed. The basin is fjord-like in its topographic setting, and is one of a series of fjord-like over-deepenings on the western flank of the Ellsworth Subglacial Highlands.

This summary of our current knowledge will document the series of radio-echo sounding (RES) transects and field campaigns from which the lake has been identified. Basal thermal regime and ice-flow conditions, which are believed to control the lake will then be described. The final section will describe future plans for the exploration of Lake Ellsworth (Lake Ellsworth Consortium, 2007).

Radio-echo sounding data

Subglacial lakes can be identified on radio-echo sounding (RES) records. RES utilizes VHF radio-waves to measure the thickness of ice sheets and suggests the presence of subglacial lakes in three ways: (1) reflections from a water surface beneath the ice are at least an order of magnitude stronger than from ice-rock contacts; (2) reflections are of constant strength across the lake, rather than the more common variable strength that returns from bedrock; (3) the surface of a subglacial lake is smooth and flat compared with the rough surrounding topography. Using these criteria enables the identification of subglacial lakes and, where more than one RES transect is available, their surface extents to be measured. Two independent airborne and two ground-based RES campaigns have identified Lake Ellsworth:

1. The first knowledge of Lake Ellsworth is reported in Siegert et al. (2004), and is restricted to one RES line, acquired in 1977–1978 (Figure 1a and b). Later RES profiles (described below) suggest that the sounding line is near-parallel to the lake long-axis, and is also near parallel to ice flow over the lake. Preliminary modeling of the lake environment suggests that the mean gradient of the lake surface reflector is 0.02, about ~11 times the ice surface slope, suggesting the lake is in hydrostatic equilibrium with the overriding ice. The slope of the ice base across Lake Ellsworth is not entirely constant; being concave over the lake's upstream side and convex across its downstream side. In other words, the ice sheet "sags" as it flows onto the lake, and buckles against the sidewall as it re-grounds. The same features have been identified over Lake Vostok and are an expected characteristic of deep-water subglacial lakes. In the cases of both lakes, the strength of the reflections from the ice-water

Vijay P. Singh, Pratap Singh & Umesh K. Haritashya (eds.), *Encyclopedia of Snow, Ice and Glaciers*, DOI 10.1007/978-90-481-2642-2,

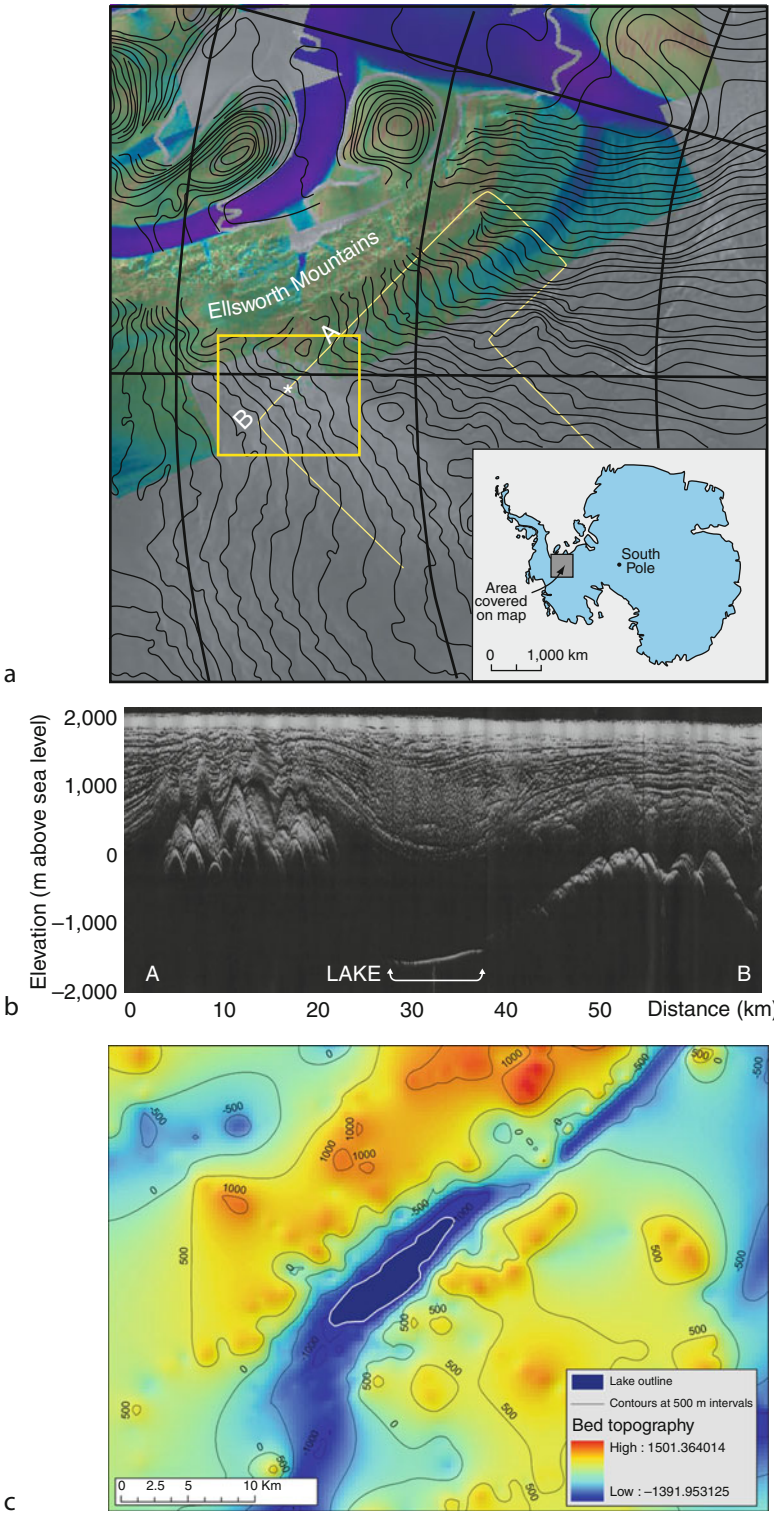

Lake Ellsworth, Figure 1 (**a**) The location of Lake Ellsworth. *Background colors* represent satellite-derived ice surface velocities (*green* = low, *purple* = high, *grey* = no data). The *yellow box* denotes bed information given in (**c**). Transect AB is provided in (**b**); (**b**) Raw 1977–1978 RES transect. The subglacial lake is located between 28 and 38 km (indicated by *arrowed line*). The pronounced slope of the lake surface is accentuated by the vertical exaggeration of the image; (**c**) Basal topography of the immediate area of Lake Ellsworth. Elevation (in meters) relative to the WGS-84 ellipsoid. Adapted from Siegert et al. (2004).

interface varies near the shores, as a consequence of the reflector's shape (Siegert et al., 2004).

2. In austral summer 2004–2005, the British Antarctic Survey flew a sounding line, using a 150 MHz ice-sounding radar, across Lake Ellsworth in the form of a bow. Part of a 35,000 km grid pattern being collected over Pine Island Glacier also crossed the lake, and identified other lake-like reflectors in the surrounding area (Vaughan et al., 2007). This suggests the lake is part of a wider subglacial drainage system. The new radar lines confirm the bright specular nature of the reflector and show a much shorter reflector than the 1977–1978 survey, of between 1.5 and 2.3 km in length. This suggests that the lake is long relative to its cross-profile, occupying a fjord-like basin on the flanks of the Ellsworth Subglacial Highlands (Figure 1c). Analysis of the RES data suggests that the ice is floating on a fluid whose density is 950–1,013 kg m^{-3}, possibly indicating that the lake is composed of fresh water (Vaughan et al., 2007).
3. In January 2006, a ground-based Chilean expedition traversed the Institute Ice Stream to Lake Ellsworth and acquired several RES transects over the lake (Vaughan et al., 2007). A 150 MHz RES system was used to collect nine lines, totaling 15 km over the lake-like reflector (Rivera et al., 2006). These lines bound the lake to the north and west, though do not constrain its upstream margins to the south and east. Here, transitional zones indicated by Rivera et al. (2006) show areas around the lake where off-line radar reflections from steep bedrock surfaces prevent the lake surface being imaged.
4. In 2007/2008 a 3-month field season, using ground-based RES and seismics, revealed the lake to be in excess of 100 m deep and confirmed it as an ideal candidate for in situ measurement and sampling. An over-snow 1 MHz ice-penetrating radar was used to acquire new radar data from Lake Ellsworth and its surroundings during 2007/2008. The survey was designed to acquire data in a grid pattern, to allow: (1) the refinement of the lake outline mapped by Vaughan et al. (2007); (2) the imaging of internal layering within the ice; and (3) the development of a digital elevation model (DEM) of the lake and the surrounding subglacial terrain. The new radar and seismic data confirms the general form of the lake outline established by Vaughan et al. (2007), but shows that Lake Ellsworth is wider and slightly longer at its downstream end than previously mapped. Internal layering is apparent within the topmost 2 km of the ice sheet overlying the lake. Localized buckling of these layers can be used to infer the direction of long-term ice flow over the lake as these structures can be traced, through a sequence of radar profiles, back to their point of origin; an area of high subglacial topography identified up-flow. Internal layering data have been integrated with the DEM of the subglacial bed to facilitate 3D numerical modeling of ice flow and basal melting over Lake Ellsworth, work that is currently in progress.

Basal thermal conditions and ice flow modeling

The basal heat flux calculated in West Antarctica from temperature gradients in boreholes is around 70 mW m^{-2} (e.g., Hulbe and MacAyeal, 1999). Numerical thermodynamic evaluations suggest that the subglacial environment above Lake Ellsworth is warm, that is, at the pressure melting point (Siegert et al., 2004). Due to increased ice thickness at the last glacial maximum (LGM), it is expected that the ice sheet was also warm based at the LGM. This indicates that Ellsworth may have existed during both the present interglacial and the LGM.

Preliminary ice flow modeling of the lake environment using internal layer architecture to invert for basal melting also suggests that the dominant process at the basal boundary condition is one of melting (Siegert et al., 2004). The model predicts that as ice flows over the lake, basal melting is expected at a rate comparable to the surface accumulation rate (which near the ice divide is ~17 cm $year^{-1}$) (Siegert et al., 2004). This melt rate is significantly greater than that calculated for Lake Vostok, though is comparable to the situation in Lake Vostok in terms of its value as a proportion of the surface accumulation rate. As melting is the driving force behind water circulation (Mayer et al., 2003), the enhanced rates of melting predicted by the model may lead to circulation in Lake Ellsworth being stronger than Lake Vostok (and many other subglacial lakes). Upstream of Lake Ellsworth, a small region of basal accretion is modeled at a rate of 20 cm $year^{-1}$. It is not yet known whether this freezing rate is real, or whether three-dimensional flow of ice (not accounted for in the model) complicates ice flow upstream of the lake and influences the internal layer structures. As the rate of water supplied to the lake is considerable, it is likely that Ellsworth is part of a wider subglacial hydrological network, feeding water into the basal environment of the Pine Island catchment.

Exploration of Lake Ellsworth

It is a well-established hypothesis that Antarctic subglacial lakes house unique forms of life and hold detailed sedimentary records of past climate change. Testing this hypothesis requires in situ examination. Of the >145 subglacial lakes known in Antarctica, Lake Ellsworth stands out as a candidate for first exploration for the following reasons (Lake Ellsworth Consortium, 2007):

- The base of the West Antarctic Ice Sheet has been accessed, sampled, and measured. Accessing Ellsworth would, therefore be less environmentally sensitive compared to accessing an East Antarctic subglacial lake.
- Lake Ellsworth is located close to the ice divide, so drilling from the ice surface into the lake will not be complicated by ice flow.

- Lake Ellsworth has been meaningfully characterized by geophysical methods.
- The sediments across the floor of Lake Ellsworth may contain a record of West Antarctic Ice Sheet history.
- The geological setting of the lake is better understood than any other Antarctic subglacial lake, as there is substantial outcrop of rock in the nearby Ellsworth Mountains.
- The ice-sheet surface elevation over Lake Ellsworth is 2,000 m above sea level; more than a kilometer lower than the ice surface over East Antarctic subglacial lakes. Altitude related problems encountered by scientists at the center of the East Antarctic Ice Sheet would not be an issue during the study of Lake Ellsworth.

A consortium of over twenty scientists from eleven institutions has been assembled to plan the exploration of Lake Ellsworth. Lake Ellsworth will be accessed using clean technology hot water drilling. Once lake access is achieved, a sterile probe will be lowered down the borehole and into the lake. The probe will contain a series of instruments to measure the lake water and sediments, and will be tethered to the ice surface through which power, communication, and data will transmit. The probe will be dropped down the water column to the lake floor. The probe will then be pulled up and out of the lake, measuring its environment continually as this is done. Once at the ice surface, any samples collected will be taken from the probe for laboratory analysis. The duration of the science mission, from deployment of the probe to its retrieval, is likely to be between 24 and 36 h. Measurements to be taken by the probe include: depth, pressure, conductivity, and temperature; pH levels; biomolecules (using life marker chips); anions (using a chemical analyzer); nitrogen isotopes (using a tuned laser diode); visualization of the environment (using cameras and light sources); dissolved gases (using chromatography); and morphology of the lake floor and sediment structures (using sonar). After the probe has been retrieved, a sediment corer will be dropped into the lake to recover material from the lake floor. The consortium plans to access Lake Ellsworth in 2012–2013.

Acknowledgments

Funding was provided by UK NERC grants NER/D008751/1, NE/D009200/1 and NER/D008638/1.

Bibliography

Hulbe, C. L., and MacAyeal, D. R., 1999. A new numerical model of coupled inland ice sheet, ice stream, and ice shelf flow and its application to the West Antarctic Ice Sheet. *Journal of Geophysical Research*, **104**(25), 25,349–25,366.

Lake Ellsworth Consortium, 2007. Exploration of Ellsworth Subglacial Lake: a concept paper on the development, organisation and execution of an experiment to explore, measure and sample the environment of a West Antarctic subglacial lake. *Reviews in Environmental Science and Biotechnology*, **6**, 161–179.

Mayer, C., Grosfeld, K., and Siegert, M. J., 2003. The effect of salinity on water circulation within subglacial Lake Vostok. *Geophysical Research Letters*, **30**(14), 1767, doi:10.1029/2003GL017380.

Oswald, G. K. A., and Robin, G. de Q., 1973. Lakes beneath the Antarctic Ice Sheet. *Nature*, **245**, 251–254.

Rivera, A., et al., 2006. Expedicion al lago subglacial Ellsworth, *Boletin Antarctico Chileno*, **25**(1), 7–11.

Siegert, M. J., Dowdeswell, J. A., Gorman, M. R., and McIntyre, N. F., 1996. An inventory of Antarctic sub-glacial lakes. *Antarctic Science*, **8**, 281–286.

Siegert, M. J., Hindmarsh, R., Corr, H., Smith, A. M., Woodward, J., King, E. C., Payne, T., and Joughin, I., 2004. Subglacial Lake Ellsworth: a candidate for in situ exploration in West Antarctica. *Geophysical Research Letters*, **31**, L23403.

Vaughan, D. G., Rivera, A., Woodward, J., Corr, H. F. J., Wendt, J., and Zamora, R., 2007. Topographic and hydrological controls on Subglacial Lake Ellsworth, West Antarctica. *Geophysical Research Letters*, **34**, L18501, doi:10.1029 /2007GL030769.

LAKE ICE

Rajesh Kumar
School of Engineering and Technology, Sharda University, Greater Noida, NCR, India

The lake ice formation takes place when the daily temperature is below the freezing point. Lake ice cover is normally

Lake Ice, Figure 1 Synoptic view of the lake ice formed on the upper surface of lake water in the Baralacha La region of Himachal Pradesh, India.

Lake Ice, Figure 2 Close view of above lake showing liquid water underneath the thin lake ice.

a seasonal phenomenon and once formed the lake ice gets thicker and thicker over the course of the winter as the temperature gets colder and colder. It starts melting in spring. The surface water of the lake freezes at 0°C while the bottom layer of water maintains at above freezing temperature.

The occurrence of lake ice is primarily a function of air temperature. Once meteorological conditions provide colder breeze over warmer water, it forms ice on the surface of water due to advection cooling. But the water below the surface of ice is not much cooled so it exists in liquid phase. Hence the lake ice is found at the lake surface only (Figures 1 and 2).

LAKE VOSTOK

Malte Thoma
Bavarian Academy and Sciences, Commission for Glaciology, Munich, Germany
Alfred Wegener Institute for Polar and Marine Research, Bremerhaven, Germany

Definition

Subglacial Lake. A lake covered by an ice sheet or glacier.

Introduction

Subglacial Lake Vostok is the largest of at least 370 (Wright and Siegert, 2010) subglacial lakes in Antarctica, and it was the first to be discovered. A lot of our knowledge about Antarctica, about the Earth's climate history, and about the subglacial lakes has been descended from the research station built at this location. This contribution summarizes some of the knowledge gained after more than 50 years of research in the heart of Antarctica, on top of, within, and below the ice.

On top of the ice: discovery

During the *International Geophysical Year*, the *Second Soviet Antarctic Expedition* encountered a quite plain area in the center of Antarctica. For the intended permanently manned station far away from any human settlement, airborne transport is indispensable, and hence this location was chosen to establish *Vostok Station*, on December 16, 1957. It is located close to the *Southern Pole of Inaccessibility* and the *South Geomagnetic Pole*. Many scientific experiments have been carried out at Vostok Station. Analyzing the results of seismic soundings, Soviet scientists had speculated about water beneath the 3,750 m thick ice sheet even in the 1960s. Further evidence of the existence of a lake was provided by radio echo sounding in the 1970s, which was confirmed later by satellite altimetry and seismic sounding (Kapitsa et al., 1996).

Subglacial Lake Vostok's area of about 16,000 km^2 can be estimated from airborne measurements and satellite imagery (Figure 1). The lake is surrounded by a bedrock-based ice sheet, and the ice flow approaches Subglacial Lake Vostok from Ridge B in the west, but is deflected southward over the lake (Figure 2). As the lake's surface is flat, it is reasonable to assume an isostatic equilibrium, that is, the ice floats on the water like an ice shelf. The observed ice surface slope over the lake is only 0.02%, leading to an elevation difference of about 50 m. However, because of the density differences between water and ice, surface ice slopes are enhanced approximately ten times at the lake–ice interface. This results in a lake surface elevation difference between the northern and southern tip of about 500 m.

In the ice: drilling and indications of life

In the 1970s, Soviet scientists started to drill ice cores in the vicinity of their station. These early boreholes were less than 1,000 m deep, but nevertheless they provided a unique climate archive. Deeper cores were drilled in 1984 and in the 1990s. The deepest core reached a depth of 3,623 m and penetrated the boundary between meteoric ice and refrozen lake ice at 3,539 m. From this ice core, a climate archive dating back 420,000 years was revealed. According to the seismic soundings, the water interface below Vostok Station is about 3,750 m deep, which means that below Vostok Station a layer of about 210 m refrozen lake water exists (e.g., Jouzel et al., 1999). Today, the deepest borehole is less than 100 m away from the lake's surface.

Subglacial Lake Vostok is an oligotrophic environment: Temperatures of about −3°C, permanent darkness, low nutrient supply, and a supersaturated oxygen level provide a hostile environment, which has been separated from any atmospheric influence since the Antarctic Ice Sheet formed millions of years ago. However, analyses of the refrozen water reveal that potential nutrients and even viable microorganisms exist in Subglacial Lake Vostok (e.g., D'Elia et al., 2009). If this is verified in the future, a so far undiscovered ecosystem on Earth can be explored. Subglacial Lake Vostok may be an extraordinary example of how life may develop under such extreme

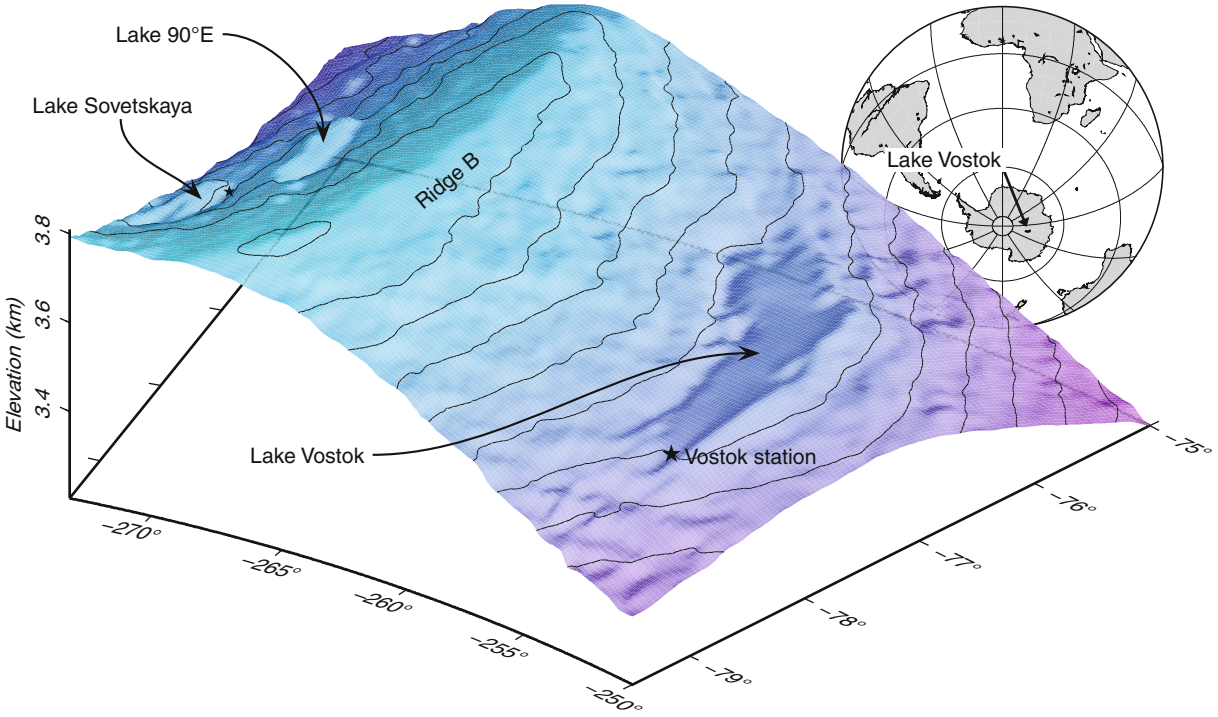

Lake Vostok, Figure 1 Lake Vostok, East Antarctica. Subglacial lakes can easily be identified by means of their flat ice sheet surface. Vostok Station is located in the southern tip of Lake Vostok. Two other major lakes can be identified across Ride B in central Antarctica: Lake 90°E and Lake Sovetskaya, named after another Russian Research station.

conditions, and this nourishes speculations about extraterrestrial life on the ice-covered Jovian moon Europa in our planetary system.

Besides life in the lake water itself, remnants of preglacial life might be stored within the sediments at the lake's bottom – at least if the lake did exist before the ice sheet formed, which is still a matter of debate (Siegert et al., 2004). After the ice formed over the preglacial lake, the supply of light, oxygen, and nutrients from the atmosphere was intercepted, leading to mass extinction. If the sediments at the lake's ground are probed, a new climate archive will be opened and information about life million years before present will be available. However, it will be problematic to probe Lake Vostok without contaminating it. According to the *observer effect*, it is impossible to sample something without changing it. In the closed subglacial system, any contamination released by a drilling equipment will permanently and irreversibly modify the lake's composition. In this sense, Lake Vostok can be interpreted as a macroscopic example of the uncertainty principle.

Because of these well-founded worries of the scientific community against a probing, Russia agreed in the late 1990s to delay the penetration of the lake until further risk assessments have been made. It is undisputed that the Russians' drilling project does not violate the *Antarctic Treaty*. Therefore, they already have filed an *Initial Environmental Evaluation*, and only the obligatory *Comprehensive Environmental Evaluation* is pending. Hence, the drilling will be legitimate. The Russians are not the only ones who have interest in probing Lake Vostok. The American Space Agency NASA has announced that they would like to test their equipment to be used on missions to other planets and moons on Earth beforehand, and that Lake Vostok would be an ideal location for this. Meanwhile, a British consortium of scientists has launched an already accepted proposal to explore and penetrate a subglacial environment at the much more accessible and tiny Antarctic Subglacial Lake Ellsworth (e.g., Woodward et al., 2010) This has stirred the somewhat calmed plans to unlock Lake Vostok again: Despite the worries and protests of scientists (e.g., Hobbie et al., 2007) and the *Antarctic and Southern Ocean Coalition* (ASOC, an environmental organization), Russian scientists reinitialized drilling during the field season 2005/2006 with an overhauled equipment and stopped the drilling only a few tens of meters close to the lake. The Russian scientists claim that they are capable of sampling lake water without infecting it with modern microbes. However, this will be quite a task as their drilling hole is filled with kerosene and other noxious fluids necessary to prevent the borehole from refreezing or from closing due to pressure forces. Technical and legal reasons have postponed the penetration of the lake so far, but the Russians have announced that after 2010 they plan to go where no man has gone before (Schiermeier, 2008).

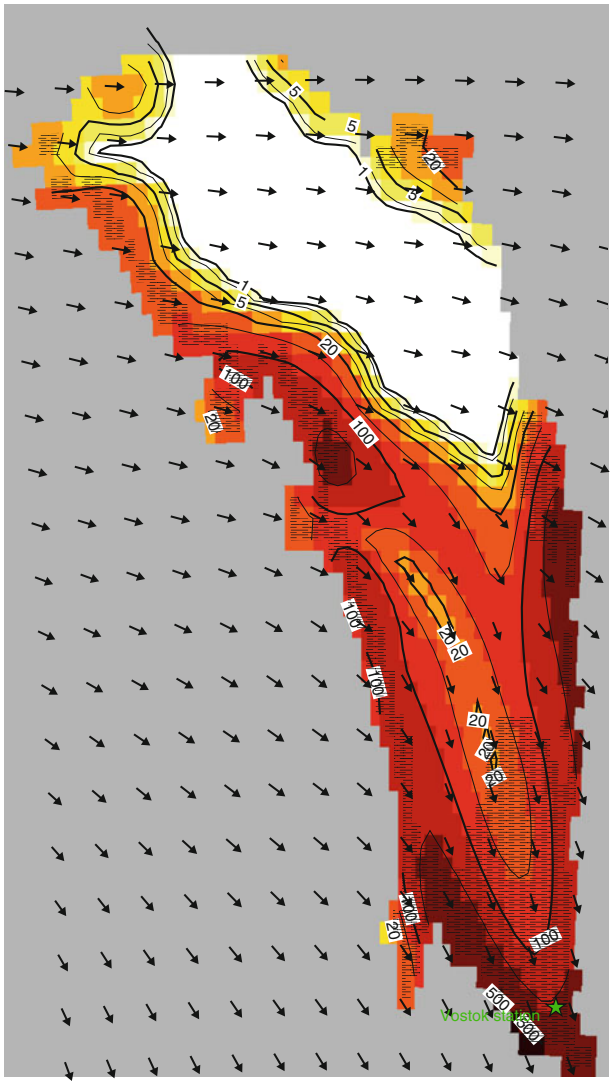

Lake Vostok, Figure 2 Modelled accreted ice distribution and its thickness (m) at the lake–ice interface (indicated by *color*) and areas where freezing takes place (*white shaded*). The surface ice flow direction (After Tikku et al., 2004) is indicated by *black arrows*.

Below the ice: modeling

The lake's area can be estimated from the surface topography, and a lot of valuable information about Lake Vostok can be gathered from the accreted refrozen lake water in the ice core. But until the lake is directly probed, detailed information about circulation and water mass exchange under the ice can only be derived from numerical modeling. From airborne gravity data and assumptions about the densities of ice, water, sediment, and rock, the lake's geometry and its water depth can be estimated (Studinger et al., 2004). In addition, seismic sounding can be used to constrain the derived geometry model (Filina et al., 2008). According to these studies, the lake's largest depth exceeds 1,000 m, the volume is about 5,000 km^3, and a sedimentary layer at the lake's bottom is several hundred meters thick.

The surface temperatures in central Antarctica are, on average, about −65°C during winter, and even in the brief summer, they barely reach −35°C. This is well below the freezing point of water, and hence ice never melts in this region of the Earth – at least not at the ice sheet's surface. Nevertheless, water does exist in its liquid form below about 4,000 m of ice. At this depth, the freezing point of fresh water is about −3°C. A small geothermal heat flux of about 50 mW/m^2, as estimated for the area of Lake Vostok, is therefore responsible (and sufficient) for melting the ice's base. Additional hydrothermal energy sources are not expected to provide energy for the melting. The meltwater is collected in the topographic basin (a rift valley according to Bell et al., 2006) forming Lake Vostok.

With this valuable information, a lake-flow model can be set up to calculate the average water circulation, the basal mass (im)balance, and the distribution of melting and freezing at the lake–ice interface (Thoma et al., 2008). These simulations show a ceaseless melting-induced ice loss of about 5×10^{-2} km^3/a, which is not balanced by freezing, and a horizontal (vertical) water velocity on the order of 1 mm/s (10 μm/s). However, the modeled low vertical velocity is a spatial average; heating from below results in upwelling of plumes that rise significantly faster (about 0.3 mm/s) to the lake's surface (Wells and Wettlaufer, 2008). The combination of the modeled basal mass balance and ice flow information allows for estimating the distribution and thickness of the accreted ice at the ice sheet base from which samples have been drilled at Vostok Station. According to Thoma et al. (2010), about 65% of the lake–ice interface is covered with accreted ice (Figure 2).

Most probably, Lake Vostok is not an isolated lake but is connected to other lakes via a subglacial network like other lakes have proven to be before (Wingham et al., 2006; Fricker et al., 2007). The water collected in the Lake Vostok basin will finally reach the Southern Ocean. The age of the lake water is estimated to be between a few thousand years and more than 100,000 years, and a more recent model-based study (Thoma et al., 2010) indicates a mean water age of about 50,000 years. However, these timescales are short compared to the Antarctic Ice Sheet's age of several million years, which means that the lake water has been replaced several times since its inception.

Conclusions

After more than 50 years of research in the heart of Antarctica, some of Lake Vostok's mysteries are revealed (like the dimension of the lake), some are depreciated (like the theory of an isolated, sealed environment), but a lot is still unknown about the massive water basin beneath the 4,000 m thick Antarctic Ice Sheet. Within the next few years, we can expect more insights to be gained from the subglacial environment, perhaps by direct sampling through an access hole.

Bibliography

Bell, R. E., Studinger, M., Fahnenstock, M. A., and Shuman, C. A., 2006. Tectonically controlled subglacial lakes on the flanks of the Gamburtsev Subglacial Mountains, East Antarctica. *Geophysical Research Letters*, **33**, L02504, doi:10.1029.2005GL025207.

D'Elia, T., Veerapaneni, R., Theraisnathan, V., and Rogers, S. O., 2009. Isolation of fungi from Lake Vostok accretion ice. *Mycologia*, **101**(6), 751–763, doi:10.3852/08-184.

Filina, I. Y., Blankenship, D. D., Thoma, M., Lukin, V. V., Masolov, V. N., and Sen, M. K., 2008. New 3D bathymetry and sediment distribution in Lake Vostok: implication for pre-glacial origin and numerical modeling of the internal processes within the lake. *Earth and Planetary Science Letters*, **276**, 106–114, doi:10.1016/j.epsl.2008.09.012.

Fricker, H. A., Scambos, T., Bindschadler, R., and Padman, L., 2007. An active subglacial water system in west Antarctica mapped from space. *Science*, **315**(5818), 1544–1548, doi:10.1126/science.1136897.

Hobbie, J. E., Baker, A., Clarke, G., Doran, P. T., Karl, D., Methe, B., Miller, H., Mukasa, S. B., Race, M., Vincent, W., Walton, D., White, J. W., and Uhle, M., 2007. *Exploration of Antarctic subglacial aquatic environments: environmental and scientific stewardship*. Washington, DC: National Academy.

Jouzel, J., Petit, J. R., Souchez, R., Barkov, N. I., Lipenkov, V. Y., Raynaud, D., Stieve-nard, M., Vassiliev, N. I., Verbeke, V., and Vimeux, F., 1999. More than 200 meters of lake ice above subglacial Lake Vostok, Antarctica. *Science*, **286**, 2138–2141, doi:10.1126/science.286.5447.2138.

Kapitsa, A. P., Ridley, J. K., Robin, G. d. Q., Siegert, M. J., and Zotikov, I. A., 1996. A large deep freshwater lake beneath the ice of central East Antarctica. *Nature*, **381**, 684–686, doi:10.1038/381684a0.

Schiermeier, Q., 2008. Russia delays Lake Vostok drill, Antarctica's hidden water will keep its secrets for another year. *Nature*, **454**, 258–259, doi:10.1038/454258a.

Siegert, M. J., 2004. Comment on "A numerical model for an alternative origin of Lake Vostok and its exobiological implications for Mars" by N. S. Duxbury, I. A. Zotikov, K. H. Nealson, V. E. Romanovsky, and F. D. Carsey. *Journal of Geophysical Research*, **109**(E02007), 1–3, doi:10.1029/2003JE002176.

Studinger, M., Bell, R. E., and Tikku, A. A., 2004. Estimating the depth and shape of subglacial Lake Vostok's water cavity from aerogravity data. *Geophysical Research Letters*, **31**(L12401), doi:10.1029/2004GL019801.

Thoma, M., Mayer, C., and Grosfeld, K., 2008. Sensitivity of Lake Vostok's flow regime on environmental parameters. *Earth and Planetary Science Letters*, **269**(1–2), 242–247, doi:10.1016/j.epsl.2008.02.023.

Thoma, M., Grosfeld, K., Smith, A. M., and Mayer, C., 2010. A comment on the equation of state and the freezing point equation with respect to subglacial lake modelling. *Earth and Planetary Science Letters*, **294**(1–2), 80–84.

Tikku, A. A., Bell, R. E., Studinger, M., and Clarke, G. K. C., 2004. Ice flow field over Lake Vostok, East Antarctica inferred by structure tracking. *Earth and Planetary Science Letters*, **227**, 249–261, doi:10.1016/j.epsl.2004.09.021.

Wells, M. G., and Wettlaufer, J. S., 2008. Circulation in Lake Vostok: a laboratory analogue study, *Geophysical Research Letters*, **35**(L03501), 1–5, doi:10.1029/2007GL032162.

Wingham, D. J., Siegert, M. J., Shepherd, A., and Muir, A. S., 2006. Rapid discharge connects Antarctic subglacial lakes. *Nature*, **440**(C6), 1033–1036, doi:10.1038nature04660.

Woodward, J., Smith, A. M., Ross, N., Thoma, M., Corr, H. F. J., King, E. C., King, M. A., Grosfeld, K., Tranter, M., and Siegert, M., 2010. Location for direct access to subglacial Lake Ellsworth: An assessment of geophysical data and modeling. *Geophysical Research Letters* **37**(L11501).

Wright, A., and Siegert, M. J., 2010. The identification and physiographical setting of Antarctic subglacial lakes: an update based on recent geophysical data. In: Siegert, M. J., Kennicutt, C., and Bindschadler, B., (eds.), Subglacial Antarctic Aquatic Environments, AGU Monograph, accepted.

Cross-references

Antarctica
Bed (Bottom) Topography
Formation and Deformation of Basal Ice
Ice Core
Ice Sheet
Ice Shelf
Lake Ice
Melting Processes
Subglacial Drainage System
Subglacial Lakes, Antarctic

LAMINATED SEDIMENTS

Rajesh Kumar
School of Engineering and Technology, Sharda University, Greater Noida, NCR, India

The laminated sediments have traditionally been considered by geologists as strata with a thickness of about less than 1 cm (Berthault, 1988). This is one of the characteristic features in the sedimentary rocks. The deposition of sediments for several years or at different geological time might have slight difference in their mineralogical composition. This exhibits different shades of colors even if they are belonging to the same area. After consolidation, these depositions in the sedimentary rocks exhibit them in the form of thin layers. Each laminated sediments or the thin layer/band represents a different phase of deposition. Lamination clusters together signify all the structures characterizing sedimentary rocks within a bed or stratum. One of the most common examples for the laminated sediments is the medium-grained reddish sandstone that possesses thin bands of red shades due to difference in iron content at each depositional phase. The ticker laminated sediments are called as bedding planes.

Bibliography

Berthault, G., 1988. Experiments on lamination of sediments. EN Technology Journal, **3**, 25–29.

LANDFORMS OF GLACIAL DEPOSITION

John F. Shroder
Department of Geography and Geology, University of Nebraska at Omaha, Omaha, NE, USA

Definition

Glacial erosion occurs in the upper, dominantly accumulation area whereas farther down near the terminus

the ice produces areas and landforms of deposition. This entry describes some of the common depositional landforms under one umbrella. For detailed description of Jökulhlaups, Moraine, and Till, please see the respective entries *Hydrology of Jökulhlaups*; *Moraine*; *Till* in this Encyclopedia.

Landforms produced by deposition of glacier materials are mainly differentiated on the basis of whether or not they are primarily ice contact or meltwater in origin. Ice contact generally means that the landform is composed dominantly of unsorted, unstratified tills, which are generally mixtures of all clast sizes from clay, silt, and sand, to cobbles and boulders. Till deposits form as *lodgement tills* through the pressure of overlying ice that consolidates them and plasters them onto the substrate beneath; the under-melt and over-melt *ablation tills* that melt out both beneath and above the ice; and *flow tills* that form from any prior tills that become water saturated and flow over other deposits and landforms. Meltwater deposits tend to be sorted and stratified. In the waning phases of the Pleistocene ice age many glaciers melted away to leave complex mixtures of various kinds of tills and glaciofluvial sediments and landforms that are collectively known as *kettle and kame topography.*

Moraine is the general term used for almost all of the landforms composed of till, and there are many kinds of moraines, depending upon where the moraine occurs in relation to the original ice that formed it and how it was formed. Thus *lateral moraines* are the long ridges that develop alongside glacier edges where sub-, en-, and supra-glacial till debris accumulates. At the terminus or front of the glacier where the mass balance of accumulation versus wastage has allowed the glacier front to remain in place for a while, some of the same processes pile up masses of till in arcuate ridges that become the *end* or *terminal moraine*. As the glacier retreats back from its farthest extent, it can form recessional moraines where the terminus holds its position for a few years. The common medial moraines that form on the surface and down inside glacier ice commonly does not hold its long, commonly sinuous landform shape once the ice melts away; instead together with other miscellaneous sources of sub-, en-, and supra-glacial debris, it becomes undifferentiated *ground moraine* that tends to be scattered about formerly glaciated landscapes. Some ground moraines become *fluted moraine* where the basal tills are scraped, squeezed, and streaked out into lineations known as "flutes."

Push moraines form where a thick glacier terminus overrides preexisting tills or glaciofluvial sediments and forces the materials bulldozer-like, up into apparent morainal forms in front of the glacier, even where some are not made only of till. Other types of moraines that are formed transverse to ice flow are *ribbed* or *Rogen moraines* that are rather irregular in shape. They can form as the result of pushing or overriding of materials reactivated by the ice, or perhaps as a transition between streamlined features up-ice and transverse forms down-ice, or where thermal transitions occur in deglaciation along the sub-ice line that can perhaps migrate on some temporally controlled basis between cold-based ice frozen to its bed and warm-based ice further toward the terminus.

De Geer moraines are much more fine or more delicate than the Rogen type and are successions of discrete narrow ridges, thought possibly to be the result of till sediments dropped out along an ice-contact sublacustrine grounding line where icebergs calved off into a lake or the sea, or where till was squeezed up. Similar *Kalixpinmo hills* or *moraines* also may be where subglacial materials are squeezed up into cavities or deformed by glacier flow.

Smooth *drumlin* forms can form from prior deposited tills that are swept over by a new ice advance that selectively erodes away surrounding tills to leave the streamlined hills behind. Drumlins are thought to form when sub-glacial meltwaters also erode the streamlined shape. Some drumlins can also have internal glaciofluvial deposits that are sorted and stratified. Together with erosional rock drumlins, it is clear that drumlin landforms are polygenetic. Finally, various crag and tail forms can occur where a glacially overridden hill can have a mass of streamlined debris drawn out behind it down-ice in a streamlined form.

Kames are a common glacial hill or ridge landform composed dominantly of glaciofluvial sediments that are deposited in a variety of meltwater environments, such as englacial, supraglacial, and proglacial environments where conditions are appropriate for accumulation of sediment. Supraglacial lakes, crevasses, the bottoms of moulin (glacial water mills), and other miscellaneous depressions are all possible localities for establishment of kames. No particular shape is implied in the designation of the polygenetic term, although those flat-topped ones that form along the margins of glaciers or across the top of the glacier by meltwater streams or lakes, commonly become *kame terraces*.

Eskers are polygenetic also and can form as long, winding ridges of glaciofluvial sediments, commonly as a result of deposition in linear subglacial and englacial streams in tunnels, as well as in supraglacial streams. In some cases, however, the depositional processes can involve deposition of glaciofluvial sediment in a series of deltas into ice-contact lakes, which as the ice front retreats, allows the delta to retreat as well, leaving behind a series of long- or short-beaded eskers.

Glacier-fed deltas associated directly with meltwaters are classified on the basis of water depth and gradients of the feeder river. Shoal or shallow water types form Hjulström types of deltas with gently sloping fronts. Steeper and slightly deeper forms are the "classic" Gilbert-type deltas with clear topset, foreset, and bottomset bedding forms. As the water deepens and the slopes vary, various subaqueous debris cones, submarine ramps, and lobes develop, commonly as a result of subaqueous mass movement.

The regions out in front of glaciers that are washed over extensively by braided meltwater streams are replete with widespread fluvioglacial sediments that in mountainous regions form *valley trains,* and in more open regions spread out as *outwash plains* or *sandars* (singular – *sandur*).

Such regions may be the product of the slow melt of glaciers in the region, or the more spectacular breakout floods due to breakage of an ice dam or because of subglacial volcanic eruptions that result in abrupt, high-discharge floods or *jökulhlaups*. Valley trains and outwash plains are commonly pocked with kettle holes result where blocks of ice melted out leaving a remnant, commonly water-filled, depression behind.

Cross-references

Glacier Lake Outburst Floods
Hydrology of Jökulhlaups
Moraine
Sediment Entrainment, Transport, and Deposition
Till

LANDFORMS OF GLACIAL EROSION

John F. Shroder
Department of Geography and Geology, University of Nebraska at Omaha, Omaha, NE, USA

Definition

Landforms produced by the glacial erosion. Glacial erosion occurs in the upper, dominantly accumulation regions beneath the ice of glacierized valleys and ice sheets and ice caps. For detailed description of various aspects, please see the following entries: *Glacial Erosion*; *Landscapes of Glacial Erosion*; *Sediment Entrainment, Transport, and Deposition*.

The characteristics of glacially eroded landforms are primarily classified into four main categories of bedrock, topography, glacial processes, and time. Bedrock controls include the actual lithologies themselves, the character and spacing of the joints, the degree of preglacial weathering, and the overall rock structure. Topographic controls of glacial erosion are constituted by the relative relief, the shape of the relief, its alignment in relation to ice flow, and the overall altitudes involved. The morphology of the ice mass and its thickness help to control landform production, as does the direction of the ice flow, the velocity of the basal ice, and the character and amount of glacial debris. The temperature of the basal ice is essential because cold-based glaciers frozen to their beds do not erode their substrates, whereas warm-based ice in association with plentiful meltwater is a highly effective erosive agent. Change of any of these factors over time will affect the character of the eroded landforms, just as does the overall length of time that the region is glacierized.

Glacial erosion occurs by a number of processes that commonly generate sequences of scale-dependent landforms as a result of direct ice contact through crushing and fracturing, plucking or quarrying, and abrasion, as well as through fluvial erosion beneath the ice. The processes of *crushing* and *fracture* of the rock beneath a glacier produce chattermarks and crescentic fractures. *Plucking* or *quarrying* occurs during regelation slip wherein meltwater migrates to the downglacier side of an obstruction and refreezes to also incorporate fractured rock into the regelation layer that the glacier then carries away. *Abrasion* occurs where small to large grains of rocks and minerals are held by the ice and dragged over the substrate to grind away at it. At the very smallest level, fine clastic abrasives beneath the ice cover can polish the rock; at slightly larger scales, *striae* or scratches result, and above that even larger grooves are cut into the rock. *Plastically molded surfaces* or *P-forms* are eroded into bedrock as sinuous rounded forms possibly formed by the action of water-saturated tills, which are forced out under pressure beneath the ice. Fluvial erosion occurs beneath warm-based glaciers that are not frozen to their beds where meltwaters can be under pressure and where they can entrain large quantities of clastic particles that act as effective erosive tools. *Subglacial channels* and *potholes* can be developed, as well as large *tunnel valleys* that can be kilometers in width and tens of kilometers in length.

Glacially eroded valleys are easy to recognize because they so commonly have a U-shaped cross section, in contrast to the more V-shaped valleys produced by running water alone. *Glacial troughs* most closely conform to a caternary curve that forms primarily through plucking and abrasion on the lower sidewalls and bottoms of the valleys. In the course of its movement down valley, the glacier commonly exploits valley-wall constrictions, differences in rock hardness, closer joint spacing directly below where a tributary glacier added to the ice discharge to enhance its erosional ability.

Glacial troughs can be carved out of winding river valleys that have interlocking spurs, in which case they will be eroded away to leave *ice-faceted spurs* or *truncated spurs* that align between the lateral valleys. Where tributary ice streams have joined the trunk ice stream, the floors of these smaller glacier troughs are generally above the floor of the main glacier valley and *hanging troughs* or *hanging valleys* form, commonly with waterfalls once the ice has melted away.

As glacial troughs are blocked by moraines, they can fill with *glacial trough lakes* that drown the valley floor. Similarly, where glaciers descended close to or below sea level, a subsequent postglacial rise in sea level has generated *glacial fiords* invaded by an arm of the sea into the submerged glacial trough.

At the head of a glacial trough commonly exists a steep-headed, half-bowl-shaped basin or *cirque* scooped out of the bedrock that forms as a consequence of intense frost action and nival processes adjacent to the ice. The flow lines in the ice in the zone of accumulation carry rock fragments down to the bedrock beneath the glacier where it becomes deeply abraded and even overdeepened through abrasion and plucking. Once the ice has melted away, a *tarn* lake can result where the water is dammed up behind the rock sill at the lip of the cirque.

As cirques and glacial troughs dissect a mountain range, the upland remnants between three or more back-to-back

cirques erode rectilinear glacial monuments, generally in flat-lying rocks, or triangularly faced *horns* in other rocks or in places where the monuments have been reduced by headward erosion from the opposing cirques. A saw-toothed ridge or divide between cirques or glacier troughs consists of low *cols* and sharp knife-edged ridges that can form an *arête*. Multiple cirques along a mountain range can form a *scalloped upland* or *biscuit-board topography*, in analogy to a layer of prepared bread dough on a pastry board with arcuate pieces cut out for biscuits that leave the cirque shape behind.

Landform eminences produced primarily by plucking and quarrying at the smaller end of the scale form streamlined *roche moutonnée* of a few meters to a few decimeters in size that tend to be plucked and rough and jagged on the down-ice or lee side, and rounder, smoother, and abraded on the up-ice or stoss side. At the large end of the scale, the same sort of streamlined landform is hundreds of meters in size and generally stands as an isolated and asymmetric rocky crag or mountain *flyggbirge*. In a few cases of completely streamlined erosional forms, *whalebacks* or larger *rock drumlins* can form. Finally, jagged mountain peaks that protrude through a surrounding ice sheet are *nunataks*, which is an Inuit word for "place of refuge."

Summary

Glacial erosion occurs most prominently in association with warm-based ice that is not frozen to its bed and in abundant association with meltwaters. Glacial erosion is accomplished primarily by subglacial abrasion from other rock fragments entrained in the moving ice, as well as by plucking in which basal meltwater refreezes beneath the ice to pull off blocks of bedrock. A wide variety of small-scale and large landforms are produced in the bedrock.

Bibliography

Benn, D. I., and Evans, D. J. A., 1998. *Glaciers and Glaciation*. London: Arnold, p. 743.

Menzies, J., 2002. *Modern and Past Glacial Environments*. Oxford: Butterworth Heinmann, p. 543.

Cross-references

Glacial Erosion
Landscapes of Glacial Erosion
Sediment Entrainment, Transport, and Deposition

LANDFORMS OF GLACIAL TRANSPORTATION

John F. Shroder
Department of Geography and Geology, University of Nebraska at Omaha, Omaha, NE, USA

Definition

Landforms produced due to the movement of glacier.

All glacial deposits were transported from other sources but landforms specific only to transportation can be considered where the mechanism of motion and its results are the most important factors to be considered. Thus features such as *erratics*, *boulder trains*, or glacial erratic *indicator fans* or *dispersal fans* are the chief landforms of glacial transportation. Such landforms are commonly recognized as exotic blocks far from their original source that will reveal paleo-flow directions of the ice once the course of transport is determined by finding the original outcrop from which they were derived.

For an erratic to be incorporated within a glacier, it is necessary either for the ice to exert enough tractive force on a block to pick it up from the bed over which it is flowing, or for the block to fall from high cliffs to the glacier surface and be carried along passively thereafter. Small blocks are brought into ice streams both ways constantly but very large blocks require unusual sets of circumstances in order to become transported landforms. A possibility can be that huge erratic blocks might be moved by cold-based glaciers if the 0°C isotherm moves down reasonably close to the glacier bed so that the block is frozen onto the overlying ice. Then, if the friction at the frozen ice/rock interface exceeds that occurring on the lower unfrozen plane of weakness in the rock or that of the substrate below, the whole block can be picked up and dragged along. Subsequently as is characteristic of cold-based glaciers, the block can rise in the ice stream as ever more material and ice is added underneath it by regelation refreezing at the glacier base.

A huge such erratic in Germany measures 4 km by 2 km by 120 m thick. Elsewhere large quartzite blocks of the Foothills Erratic Train occur on the prairie underlain by Cretaceous bedrock in Alberta, Canada, more than 375 km from their source in the mountains of Jasper National Park. The largest of these erratic blocks, the Okotoks erratic near Calgary, is thought to weigh about 16,000 t.

Erratic trains can be divided into two chief types: the *Dubawnt type* in which erratic blocks are spread as a plume down-ice from a relatively restricted source outcrop; and the *Boothia type*, which on the other hand is a boulder train characterized by erratic plumes that extend out from small parts of large source areas by ice streams of more rapid flow within an ice sheet. In general, no matter which type of erratic train is involved, the dispersal patterns of the erratics can be used to reconstruct former ice transportation pathways. Care must be exercised in interpretation, however, because debris transport histories may involve several cycles of glaciations during which time ice divides and ice-flow vectors may shift altogether from one direction to another, even as much as 90° or more. In general, most boulder trains are fan-shaped down-ice, although some may be rather rectilinear in the shape of their edges.

In those rare cases where a medial moraine from a glacier is preserved on the ground after the glacier has melted away, a clear transportation landform results.

For example, in the case of medial moraines that derive from a nunatak mountain that projects through an ice sheet, the erratic debris spread out from that nunatak while the ice is in place will form a more-or-less vertical debris septum within the ice that exists as a medial moraine on the surface of the ice. If the ice melts away without too much meltwater removal of the debris, a linear pile of boulders and moraine hills will show the original transportation direction.

Summary

All glacial deposits were transported from somewhere else but only a few show clear evidence of transportation that sets them apart from the others. Thus, glacial landforms of transportation include single erratics, boulder trains of erratics, and indicator fans or dispersal fans. More rarely, medial moraines may be preserved.

Bibliography

Benn, D. I., and Evans, D. J. A., 1998. *Glaciers and Glaciation*. London: Arnold, p. 743.

Menzies, J., 2002. *Modern and Past Glacial Environments*. Oxford: Butterworth Heinmann, p. 543.

Cross-references

Glacier Motion/Ice Velocity

LANDSCAPES OF GLACIAL EROSION

Martin P. Kirkbride
Geography, School of the Environment, University of Dundee, Dundee, Scotland, UK

Definition

A landscape of glacial erosion is one in which a large part of the landscape comprises exposed glacially molded bedrock, evidence of the net removal of rock by glacier abrasion and quarrying. Landscapes comprise erosional landforms at scales from centimeters to kilometers. This entry discusses the significance of these landscapes and their role in landscape evolution beneath ice sheets and alpine glaciers. For detailed description about landforms and glacier erosion, please see following entries: *Glacial Erosion*; *Landforms of Glacial Erosion*, etc.

A new realization of the significance of glacial erosional landscapes

Glaciers have been recognized as potent agents of landscape modification since the earliest days of classical Glacial Theory. At the landscape scale, understanding glacial topography was for many decades limited to sterile descriptions of form, because a physical understanding of subglacial erosion processes was insufficiently advanced to explain landform assemblages at landscape scales. Furthermore, the impossibility of deriving direct chronological information from denuded bedrock landscapes precluded any empirical attempt to construct evolutionary models of erosion-dominated landscape development. All this changed in the late twentieth century due to advances in four areas of science: (1) the development of powerful numerical models of glacier and ice sheet behavior; (2) application of new techniques for estimating denudation rates in eroded landscapes, notably thermochronometry and cosmogenic isotope analysis; (3) better understanding of subglacial erosion, notably the integration of basal water pressure variations into explanatory models, and (4) high-resolution proxy records of global climate history from ice cores and marine sediments, which could be used to drive computer models of glacier and ice sheet behavior. Recent research attempts to integrate glaciological and geomorphological models to "recreate" glacial erosional landscapes. Their outputs can then be measured against real landscapes and empirically calculated rates of glacial erosion and topographic change. These advances allow long-standing questions in glacial geomorphology finally to be addressed, such as:

What do the preserved landscapes of former ice sheet beds tell us about the life cycles of ice sheets?
How long does it take for glacial topography to form on a previously unglaciated landscape?
What are the relative rates of fluvial and glacial erosion at landscape scales of space and time?
What role do glaciations play in the uplift and evolution of mountain ranges?

Modeling glacial landscape evolution using coupled ice-bedrock models takes two approaches. Forward modeling shows how an initial unglaciated landscape is modified by ice cover (e.g., Jamieson et al., 2008): reverse modeling starts with current terrain models and works backward to "recreate" the preglacial landscape (e.g., Jamieson et al., 2005). Armed with these techniques, studies of glacial landscape evolution are now contributing to wider debates involving the roles of ice sheets and of alpine mountain building in global climate change.

Classification and origins of erosional landscapes under ice sheets

Sugden and John (1976) classified glacial erosional landscapes at continental scales according to the role of thermal regime in promoting or inhibiting erosion, and to the consequent character of the deglaciated terrain (Table 1). The main landscape types of areal scouring, selective linear erosion, and little or no erosion, are primarily related to spatial variations in thermal regime (Sugden, 1974, 1978). Areal scouring creates distinctive landscapes of exposed bedrock in the form of rock basins, roches moutonées, and other more-or-less streamlined forms reflecting former ice flow. Though often limited to low-relief landscapes, areal scouring of uplands (including summits) should also be included in the landscape type where the terrain was inundated by an ice sheet moving across the area from a distant source.

Landscapes of Glacial Erosion, Table 1 Classification of landscapes of glacial erosion (After Sugden, 1974; Sugden and John, 1976; Summerfield, 1991; Benn and Evans, 1998)

Landscape type	Thermal regime	Topography	Examples
Areal scouring	Warm-based	Landscape dominated by exposed, plucked, and abraded bedrock forms whose scale depends on joint and fault density. Rock basins, roche moutonées, streamlined erosional forms, and striated pavements. Negligible glacial sediment cover and disorganized post-glacial drainage. Erosion aided by impermeable bedrock.	NW Scotland W Baffin Island, Canada
Selective linear erosion	Warm-based over valleys, cold-based over interfluves	Glacial modification of pre-existing fluvial valleys into troughs. Largely unmodified plateaux and interfluves may retain delicate non-glacial landforms (patterned ground, regolith)	Cairngorm Mountains, Scotland Trollaskagi Peninsula, N Iceland Beartooth Mts, Montana, USA E Greenland
Little or no erosion	Cold-based	Preglacial slope forms survive with regolith cover. Presence of former glacier cover may itself be contentious. Limited evidence of meltwater activity during deglaciation. Erosion may partly be suppressed by permeable bedrock.	NE Scotland W Sweden E Baffin island (Canada)
Alpine landscapes	Warm-based in valleys	Cirques line sharp-crested mountain ranges above glacially modified troughs, with periglacial morphogenesis on high ice-free slopes. Predominance of steep terrain with avalanche couloirs supplying much glacial accumulation.	Southern Alps (New Zealand) European Alps Southern Alaskan coast ranges

Landscapes of selective linear erosion are specific to mixed-regime ice sheets under which thin ice over uplands remains cold-based while thick ice over valleys slides under a warm-based regime, often aided by flow convergence from surrounding uplands. Valleys are deepened and reshaped to "U"-shaped trough forms, often exploiting geological weaknesses. Landscapes of little or no erosion may be controversial, because evidence of former cold-based glaciation may be elusive, and preservation of preglacial landforms and sediments may suggest ice-free conditions throughout the Quaternary.

This classic partitioning of glacial landscapes underpins all the more recent research exploring the thermomechanical controls on glacial erosion at large spatial scales. The modern challenge is to upscale process explanations of abrasion and plucking (Boulton, 1979; Hallet, 1979, 1996) to provide models of landscape evolution under ice sheets at continental scales. The challenge has been approached both empirically (Sugden, 1978; Li et al., 2005; Phillips et al., 2006; Swift et al., 2008) and theoretically, using coupled ice-sheet-erosion computer models (Hildes et al., 2004; Jamieson et al., 2008). An up-to-date summary of the fundamental controls on glacial erosion is provided by Jamieson et al. (2008). In summary, effective abrasion and quarrying require that ice is moving over the glacier bed, in turn requiring water to be present at the bed. This requires a temperate thermal regime, due to an excess heat supply to basal ice from some combination of geothermal heat flux (especially under insulating very thick ice), frictional heating by flowing ice, and heat advection by flow convergence. How effectively the resulting basal water then promotes sliding depends on another set of factors including substrate properties, water pressure variations, bed permeability, and the connectivity of the subglacial drainage network and its seasonal evolution. These factors interact on glacier beds of widely differing lithology and topography to give a challenging modeling environment. Thus, empirical observations of former ice sheet beds are vital for defining boundary conditions and geomorphological outcomes.

Former ice sheet beds show strong patterns in the distribution of glacial erosion, evidenced by landscape types, and indicative of past ice sheet thermal regime and flow structure. Earlier representations of ice sheets as defining first-order radial zones of thermal regime, erosion, and deposition (Sugden and John, 1976; Sugden, 1978) have been refined to integrate the role of dynamic ice streams evacuating ice from ice-drainage basins within ice sheets. These operate, perhaps intermittently, when thermal, substrate and hydrological conditions combine to provide conditions facilitating optimum sliding and erosion. Such palaeo-ice streams are now being recognized from their distinct geomorphological signatures. For example, in Scotland, the late Pleistocene Minch ice stream drained much of NW Scotland out to the continental shelf edge (Stoker and Bradwell, 2005) and the Strathmore ice stream concentrated ice discharges from the south and east Highlands (Golledge and Stoker, 2006). The erosional landscapes of the hinterlands and main axes of such ice streams are important evidence of their significance for the dynamics of Pleistocene ice sheets.

Alpine glacial erosion and the height of mountains

Alpine landscapes of glacial erosion are assemblages of familiar (though sometimes poorly understood) forms

including cirques, horns, arêtes, and troughs, with the common characteristic of local accumulation sources and erosion by partly or entirely warm-based cirque and valley glaciers. As a result, alpine landscapes are best developed in mid-latitude mountain ranges.

The significance of alpine erosional topography for tectonic-isostatic modeling of mountain uplift highlights another example of a renewed scientific interest in "old-fashioned" glacial landscapes. Molnar and England (1990) highlight the feedbacks between the glacial denudation of mountain ranges and their uplift. Isostasy compensates for the majority of the crustal thickness lost to erosion of the mountains. Thus, removing 60 m of crust from range crests would lower the mountains by only c. 10 m. Molnar and England provocatively suggest that if the erosion was focused along valleys, and the isostatic response was areally distributed, this could lead to an increase in summit elevations, greater ice cover, and more erosion. Paradoxically, deepening of glacial troughs during glacial cycles could thereby increase the maximum height of alpine mountains even if average relief did not change. They hint that the initiation of Quaternary glaciations could thereby have accelerated mountain-building processes due to climatic change.

This controversial idea has been countered by the "glacial buzzsaw" hypothesis (Brozović et al., 1997). This depends on a premise that glacial erosion in alpine terrain is more effective than fluvial erosion, as several authors including Montgomery (2002) have argued. As a mountain massif is uplifted above the glaciation threshold, trough cutting will accelerate mass loss from the uplifting crust while cirque development and periglacial slope mass-wasting will "shave off" the summits to limit range heights. Where summits intersect the glaciation limit by only enough to produce cirque glaciers, cirque evolution primarily by lengthening more than by deepening or widening (Brook et al., 2006a) means that retreating headwalls on opposing slopes may lower the ridgelines. A negative feedback is hypothesized, in which the taller and steeper the mountains, the more erosive the glaciers, so that the height of mountain ranges becomes self-limiting. This mechanism has been suggested to explain range hypsometry and/or long-term sediment yields in the Himalaya (Brozović et al., 1997) the Andes (Montgomery et al., 2001), Alaska (Spotila et al., 2004), and the Western Cordillera of North America (Mitchell and Montgomery, 2006; Foster et al., 2008). Evidence for the buzzsaw also includes systematic relationships between both equilibrium-line altitudes and range crests (Porter 1964), and between ELA and maximum ice flux and erosion (Foster et al., 2008). The buzzsaw hypothesis can be criticized for an overreliance on the hypsometric (area-altitude) distribution of relief. In the European Alps, for example, uplifted preglacial valley floors below glacially modified peaks could be mistaken for "buzzsaw" planation. The applicability of the buzzsaw hypothesis to different tectonic and climatic settings is an area for further research.

Landscape modification over multiple glacial cycles

How long does it take to establish a glacial erosional landscape on initially unglaciated terrain? Modeling of trough cross-sectional development showed that a mature "U"-shaped valley can develop within a single glacial cycle of c. 10^5 years (Harbor et al., 1988). In New Zealand's Southern Alps, empirical verification for this estimate is provided by examining the erosional geomorphology of mountains in which trough-and-arête topography evolved on uplifting ranges exposed to glaciations for only the last 200,000 years of glacial duration (Kirkbride and Matthews, 1997; Brook et al., 2006b). These studies imply that mature troughs can be established early in a succession of glacial cycles in tectonically active maritime mountain ranges, where glacial erosion rates are of the order of at least several millimeters per year. Glacial landscape evolution would be correspondingly slower where low erosion rates (c. 0.01–0.1 mm/year) occur in dry climates and on durable crystalline rocks. On geological timescales, erosive alpine glaciers can impose glacial landscapes on the Earth's crust very rapidly. Later glaciations presumably contribute little to further topographic evolution once valley cross sections are adjusted to efficiently evacuate ice discharges. Long-term feedbacks between glacial landscape evolution and ice extent are suggested by Kaplan et al.'s (2009) observation that Patagonian glaciations were of successively smaller magnitude over the last 1.1 million years, in spite of favorable climate, as glacial erosion reduced potential ice accumulation areas and provided a topography favoring low-gradient fast ice flow.

Conclusions

Glacial modification of topography is important in two main respects. First, understanding how glacial erosion operates at landscape scales allows reconstruction of past basal processes beneath continental ice sheets, helping to understand ice sheet evolution and response to climate change. Second, erosional landscapes in alpine mountain ranges have a characteristic hypsometry and elevated sediment yield that feeds into models of mountain uplift and denudation. The study of landscapes of glacial erosion has progressed remarkably over several decades from bland description of form and topography to being an integral component of modeling climate-tectonic interactions in Earth system science.

Bibliography

Benn, D. I., and Evans, D. J. A., 1998. *Glaciers and Glaciation*. London: Arnold, p. 734.

Boulton, G. S., 1979. Processes of glacial erosion on different substrata. *Journal of Glaciology*, **23**, 15–37.

Brook, M. S., Kirkbride, M. P., and Brock, B. W., 2006a. Cirque development in a steadily uplifting range: rates of erosion and long-term morphometric change in alpine cirques in the Ben Ohau Range, New Zealand. *Earth Surface Processes and Landforms*, **31**, 1167–1175.

Brook, M. S., Kirkbride, M. P., and Brock, B. W., 2006b. Quantified timescale for glacial valley cross-profile evolution in alpine mountains. *Geology*, **34**, 637–640.
Brozović, N., Burbank, D. W., and Meigs, A. J., 1997. Climatic limits on landscape development in the northwestern Himalaya. *Science*, **276**, 571–574.
Foster, D., Brocklehurst, S. H., and Gawthorpe, R. L., 2008. Small valley glaciers and the effectiveness of the glacial buzzsaw in the northern Basin and Range, USA. *Geomorphology*, **102**, 624–639.
Golledge, N. R., and Stoker, M. S., 2006. A palaeo-ice stream of the British ice sheet in eastern Scotland. *Boreas*, **35**, 231–243.
Hallet, B., 1979. A theoretical model of glacier abrasion. *Journal of Glaciology*, **23**, 39–50.
Hallet, B., 1996. Glacial quarrying, a simple theoretical model. *Annals of Glaciology*, **22**, 1–8.
Harbor, J. M., Hallet, B., and Raymond, C. F., 1988. A numerical model of landform development by glacial erosion. *Nature*, **333**, 347–349.
Hildes, D. H. D., Clarke, G. K. C., Flowers, G. E., and Marshall, S. J., 2004. Subglacial erosion and englacial sediment transport modelled for the North American ice sheets. *Quaternary Science Reviews*, **23**, 409–430.
Jamieson, S. S. R., Hulton, N. R. J., Sugden, D. E., Payne, A. J., and Taylor, J., 2005. Cenozoic landscape evolution of the Lambert basin, East Antarctica: the relative role of rivers and ice sheets. *Global and Planetary Change*, **45**, 35–49.
Jamieson, S. S. R., Hulton, N. R. J., and Hagdorn, M., 2008. Modelling landscape evolution under ice sheets. *Geomorphology*, **97**, 91–108.
Kaplan, M. R., Hein, A. S., Hubbard, A., and Lax, S. M., 2009. Can glacial erosion limit the extent of glaciation? *Geomorphology*, **103**, 172–179.
Kirkbride, M., and Matthews, D., 1997. The role of fluvial and glacial erosion in landscape evolution: the Ben Ohau Range, New Zealand. *Earth Surface Processes and Landforms*, **22**, 317–327.
Li, Y., Harbor, J., Stroeven, A. P., Fabel, D., Klemen, J., Fink, D., Caffee, M., and Elmore, D., 2005. Ice sheet erosion patterns in valley systems in northern Sweden investigated using cosmogenic nuclides. *Earth Surface Processes and Landforms*, **30**, 1039–1049.
Mitchell, S. G., and Montgomery, D. R., 2006. Influence of a glacial buzzsaw on the height and morphology of the Cascade Range in central Washington State, USA. *Quaternary Research*, **65**, 96–107.
Molnar, P., and England, P., 1990. Late Cenozoic uplift of mountain ranges and global climate change: chicken or egg? *Nature*, **346**, 29–34.
Montgomery, D. R., 2002. Valley formation by fluvial and glacial erosion. *Geology*, **30**, 1040–1050.
Montgomery, D. R., Balco, G., and Willett, S. D., 2001. Climate, tectonics, and the morphology of the Andes. *Geology*, **29**, 579–582.
Phillips, W. M., Hall, A. M., Mottram, R., Fifield, L. K., and Sugden, D. E., 2006. Cosmogenic ^{10}Be and ^{26}Al exposure ages of tors and erratics, Cairngorm Mountains, Scotland: timescales for the development of a classic landscape of selective linear glacial erosion. *Geomorphology*, **73**, 222–245.
Porter, S. C., 1964. Composite Pleeistocene snowline of Olympic mountains and Cascade range, Washington. *Geological Society of America Bulletin*, **75**, 477–482.
Spotila, J. A., Buscher, J. T., Meigs, A. J., and Reiners, P. W., 2004. Long-term glacial erosion of active mountain belts: example of the Chugach-St.Elias ranges, Alaska. *Geology*, **32**, 501–504.
Stoker, M., and Bradwell, T., 2005. The Minch palaeo-ice stream, NW sector of the British-Irish ice sheet. *Journal of the Geological Society*, **163**, 425–428.
Sugden, D. E., 1974 Landscapes of glacial erosion in their relationships to ice, topographic and bedrock conditions. *Institute of British Geographers, Special Publication* 7, pp. 177–195.
Sugden, D. E., 1978. Glacial erosion by the Laurentide ice sheet. *Journal of Glaciology*, **20**, 367–391.
Sugden, D. E., and John, B. S., 1976. *Glaciers and Landscape*. London: Arnold.
Summerfield, M. A., 1991. *Global Geomorphology*. Longman: Harlow, p. 537.
Swift, D. A., Persano, C., Stuart, F., Gallagher, K., and Whitham, A., 2008. A reassessment of the role of ice sheet glaciations in the long-term evolution of the East Greenland fjord region. *Geomorphology*, **97**, 109–125.

Cross-references

Alps
Andean Glaciers
Cirque Glaciers
Glacial Erosion
Glacial Geomorphology and Landforms Evolution
Himalaya
Landforms of Glacial Erosion
Subglacial Processes
Temperate Glaciers

LAST GLACIAL MAXIMUM GLACIATION (LGM/LGP) IN HIGH ASIA (TIBET AND SURROUNDING MOUNTAINS)

Matthias Kuhle
Department of Geography and High Mountain Geomorphology, Geographical Institute, University of Göttingen, Göttingen, Germany

Synonyms

Pleistocene glaciation of High Asia during the last ice age; Quarternary glaciation of High Asia during the MIS 3-2

Definition

Reconstruction of the maximum extent of the ice cover in High Asia.

Introduction: The state of research up to 1973

A synopsis of older results and views on the Pleistocene glacier cover in High- and Central Asia has been provided by Wissmann's (1959) compilation. Glacier cover of Tibet is discussed in the Chinese literature by Shi and Wang (1979), and has also been reproduced by CLIMAP (Cline, 1981, entitled "Last Glacial Maximum"). These authors speak of a 10% to maximum 20% ice cover of the mountains and plateaus of Tibet. Even in the "Quaternary Glacial Distribution Map of Qinghai-Xizang (Tibet) Plateau" (Shi et al., 1991), this opinion is to a great extent repeated and supported. However, there was a first restriction: Zhou Shangzhe, a member of this group, agreed with the author's reconstruction of an inland ice as for the Tibetan plateau area on Animachin (cf. Figure 1) (Kuhle, 1987, 1988a). In this map, he put down a plateau glacier area of still 400 × 300 km in size. But time and time again, from as long ago as the turn of the nineteenth to twentieth

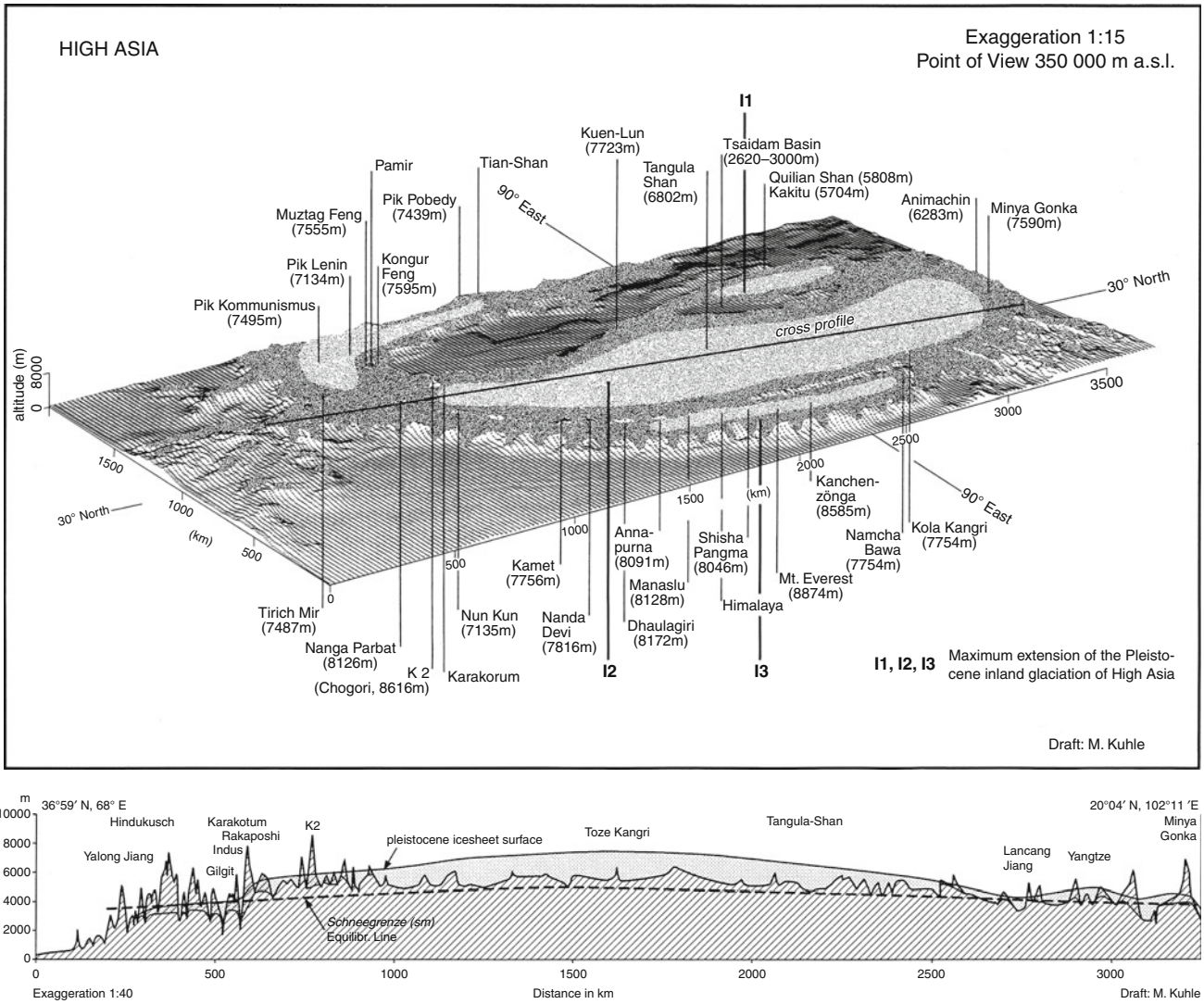

Last Glacial Maximum Glaciation (LGM/LGP) in High Asia (Tibet and Surrounding Mountains), Figure 1 *Top*: The reconstructed 2.4 million square kilometres ice sheet or ice stream network covering the Tibetan plateau (Kuhle, 1987, 1988a, b, 1989, 1995, 1998, 2001, 2004, 2005, 2007, 2011), with the three centers I 1, I 2, I 3. Only peaks higher than 6,000 m rise above the ice surface. *Figure 1. Bottom*: Cross profile of the central ice sheet from Hindu Kush in the west to Minya Gonka in the east.

century, there have been single investigators, such as Oestreich (1906), Dainelli and Marinelli (1928), Norin (1932), and others (see Kuhle, 1988b:416–417), who described ancient ice margin sites scattered throughout the high regions of Asia. According to the author's calculations, the above work represents ELA (equilibrium line altitude) depressions of more than 1,000 m and indicates, locally, significantly more glacier cover than the Wissmann scheme had acknowledged. However, these authors neither drew nor gave voice to such conclusions. Other early researchers, such as Huntington (1906), Tafel (1914), Trinkler (1932), Zabirov (1955), and others (see Kuhle, 1988b: 416–417), making more or less direct use of the data they obtained by observation, reconstructed larger glacier areas which, depending on the altitude of the mountains of plateaus, had built up only a few hundred meters of ELA depression.

The author has been fortunate in being able to carry out about 37 expeditions and research visits since 1973, some of which extended to 7 months, with the purpose of reconstructing the extent of glaciers in Asia during the glacial periods. The location and large number of areas under investigation permit reconstuction of the glacier areas to be made for the whole Tibet and parts of Central Asia. Reconstructions are supported by data from some earlier authors (see above) and are in glaring contrast to the negligible ice cover published by CLIMAP as late as 1981 (Cline, 1981) and the "Quaternary Glacial Distribution Map of Qinghai-Xizang (Tibet) Plateau" (Shi Yafeng et al., 1991). For example, the extent of glaciation of Tibet

during the Last Ice Age is given as approximately 2.4 million km² and is estimated to include a central thickness of about 2 km. Breaking up on the edges, ice discharged through the surrounding mountains as steep outlet glaciers (a.o., Kuhle, 1989, 1998, 2005).

Synopsis of the extent of the inland-ice in Tibet since the earliest Last Glacial Period (LGP)

Figure 1 shows the reconstruction of the maximum glaciation in Tibet, with an area of about 2.4 million km². In the central part, it formed a compact inland ice sheet with outflows that descended through the surrounding mountains and terminated at the steep edges of the high plateau.

To err on the safe side, the 50–70 m high, glaciofluvial gravel terraces east of 84°–85°E, which lie there on a valley floor at 3,800–3,900 m a.s.l, are classified as High Glacial deposits (Kuhle, 1989, 1998, 2004). They indicate a glacier-free Tsangpo section, which separates glacier complexes I3 and I2 as far west as 84°E (Figure 1, top).

Further in the west, the complexes I2 and I3 join again during the maximum of the Last Glacial Period (LGP) (Figure 1, top). With an equilibrium line as low as 600 m below the average plateau altitude (Figure 1, bottom), glaciation seems likely, even in the case of the more easterly Tsangpo section. This would place the gravel terraces and varved clays of the deepest parallel valleys in the late Last Glacial Period (LGP). Thus until now, at least for one time-interval during the LGP, this valley section is regarded as free of ice. A precise dating of the terraces is to be done (Figure 1, top, from north of Shisha Pangma to near Kola Kangri; cf. Kuhle, 2004). The second ice free area is the Tsaidam Depression. In the block diagram of Figure 1 (top), it shows up as narrow strip below I1 (cf. Kuhle, 2004).

Dates of lake sediments in the area of the former ice sheet are all younger than 13,000 years old because they developed only after the glaciers had melted (Gasse et al., 1996, and others). By contrast, lakes in nearby, nonglaciated areas such as the Tsaidam basin (Figure 1) and the Gobi desert display continuous sediment records going back more than 40,000 years (Pachur and Wünnemann, 1995; and others).

In a north-westerly direction from Mt. Everest to K2 (Figure 1), and from Dhaulagiri to the western Kuen Lun (Figure 1), the cross section shows that the Last Glacial Period (LGP) Equilibrium Line Altitude (ELA) runs parallel to the present ELA (in the area of southern Central Tibet the ELA attained an altitude of over 4,700 m a.s.l. (Figure 1, bottom)) (Kuhle, 1998, 2004). Nonetheless, a Last Glacial Period (LGP) Equilibrium Line Altitude (ELA) depression of at least 1,200 m means that 83–86% of the plateau surface was above the ELA. The accumulating ice necessarily led to the filling of valleys that incised the Tibet plateau. The remainder accounts for the remaining 14–17%.

Last Glacial Period (LGP) glaciers attained an approximate thickness of 2,700 m. Glacier thicknesses, ascertained by means of abrasions, polishings, and erratics, reach 1,600–2,000 m in the Himalaya and 700–1,200 m in Central and North Tibet. In the northern, southern, and western Karakorum, thicknesses of 1,750–2,600 m have been observed (Kuhle, 1987, 1988a, b, 1989, 2004, 2005) and in some places confirmed by Hewitt (2009a, b). However, these are probably minimum values. The ice may well have risen to 2,500–3,000 m in Central Tibet owing to a compact ground plan that extended over 1,500 × 3,000 km. The high viscosity of cold, continental glacier ice with annual temperatures of around −6°C to −10°C at the ELA (Kuhle, 1998) supports the build-up of ice, provided that there is sufficient precipitation. An average thickness for all of the Tibet ice of approximately 1,000 m implies that 2.2 million km³ of water was bound in the ice sheet of Tibet. This corresponds to a lowering of sea level of about 5.4–6.5 m (Kuhle, 1998).

Earlier it has been shown (cf. Kuhle, 1998, Figure 22) how the glaciated area in Tibet and in the Karakorum relates to an ELA depression or an uplift of the plateau- and mountain relief of only 500 m. At the same time, it permits an estimation of conditions if the equilibrium line drops by 1,200 m and makes the cupola-shaped build-up of the inland ice to a considerable thickness plausible. With the ice held back by mountain barriers, build-up was assisted by the low run-off, and initially by freezing to the subsurface. At a later stage, due to ice build-up, the pressure-induced melting point was reached. Run-off from the central inland ice sheet gradually increased until an equilibrium had been achieved. This was the end of ice build-up.

Meanwhile the Tibetan ice is confirmed by different disciplines. This will be shown by only three selected items

Breakdown of the summer monsoon, strengthening of the winter monsoon, and pioneering role of the subtropical inland ice

A Tibetan inland ice must have prevented the development of a low-pressure cell, a heat low, as it exists today over the heated debris covers of Tibet. Accordingly, the summer monsoon weakened. In the meantime, deep-sea cores from the Arabian Sea prove the glacial breakdown of the SW-Indian summer monsoon via dust fall (Sirocko et al., 1993). Loess-palaeosol sequences in China showing the fluctuations of the East-Asian monsoon also confirm the dramatical weakening of the summer monsoon during glacial phases (Rutter and Ding, 1993). At the same time, however, the winter monsoon strengthens during the ice ages like a mirror image of the summer monsoon. The winter monsoon was the result of differences in temperature, in this case between cold continental and catabatic winds of the Tibetan ice and the relatively warm air over the Pacific and Indian oceans. The resulting cold/dry anticyclonic wind blew loess out of the Inner-Asian glaciolimnical meltwater pits and deposited it on the Chinese loess plateau. Due to grain-size measurements in loess–palaeosol sequences, evidence was provided of

monsoonal variations and a special intensity of the winter monsoon during the glacial period (Xiao et al., 1995). Modeling has shown that the Nordic inland ices have nearly no effect on monsoon circulation whose intensity is primarily controlled by direct insolation at low altitudes (Felzer et al., 1998). Hence, the weakening of the summer monsoon and simultaneous strengthening of the winter monsoon is a clear pointer to a large-scale subtropical glaciation on the Tibetan plateau (Anderson and Prell, 1993). At the same time, this enormous climate-ecological influence on the monsoon makes clear that the Tibetan inland ice must have had a central influence on the global atmospheric circulation and energy balance. Probably, this climate-ecological signal is even strong enough to recognize a decisive influence on the global tendency towards glaciation. Tibet may have been the pacemaker and trigger for the ice ages (Kuhle, 1988a; cf. Ice age development theory, in this volume). Tibet's key role is confirmed by computer models showing that the Tibetan ice sheet is not only the first to be built up at the onset of a glacial cycle, but that when the build-up of the Tibetan inland ice had already come to an end, only half of the Nordic lowland ices were built up, i.e., that they develop much more slowly. The global ice volume then measured only 50% of the maximum ice volume during the LGM (Marsiat, 1994).

Glacial isostasy

Glacial-isostatic rebound during inter- and postglacial periods is an indicator of a High Glacial inland ice cover. The very high uplift rate of 12 mm per year measured on the Tibetan plateau (Hsu et al., 1998) is such a glacio-isostatic indicator because its value lies far above that of normal tectonic uplift. Just within the short Pleistocene period (1,000,000 years), it would lead to an unrealistic uplift of 12 km. These measurements confirm corresponding uplift calculations of the applicant due to meanwhile self-glaciated end moraines N of Shisha Pangma (S-Tibet) (Kuhle, 1995). The thickness of the inland ice of 2,000 m led to a glacio-isostatic lowering of the plateau by 600–700 m down to c. 4,300 m a.s.l. At the same time, this is the cause of the interglacial deglaciation of Tibet (Kuhle, 1995). On the basis of changes of geoid anomaly in relation to gravity anomaly – a method that allows to distinguish glacio-isostatic from tectonic uplift – also Kaufmann and Lambeck (1997) and Wang (2001) have shown a glacio-isostatic uplift of Tibet and thus have confirmed a Tibetan glaciation (Nesje and Dahl, 2001:127). Obviously, the effects of an up to 2,000 m thick ice sheet on the height of the plateau are so profound that the satellite missions CHAMP and GRACE were able to identify them (Kuhle, 2001).

Computer models and tests of general circulation models

Up to now, the general circulation models made up and tested by computer modeling were based on the global inland ice configurations of CLIMAP (1981) and COHMAP (1988), i.e., they did not include the glaciation of Tibet. These climate models unanimously show the tendency of Tibet to develop a permanent snow cover and thus to form a large-scale glaciation of the Tibetan plateau (Kutzbach et al., 1998). All sensitive experiments also indicate the growth of an ice sheet in Central Tibet which is much more likely and the development of which must have set in much earlier than that of the more northern Laurentide- and Fenno-Scandinavian ice sheets (Verbitsky and Oglesby, 1992; Marsiat, 1994). Marsiat also shows that on conditions of a reduced glaciation of Tibet, the development of the Nordic lowland ices is insignificant, too (Marsiat, 1994). This independent modeling result has been considered to be an unexpected mistake of these climate models (Verbitsky and Oglesby, 1992; Marsiat, 1994; Kutzbach et al., 1998). Actually, however, it is a clear confirmation of the terrestrial field data (Kuhle, 1987, 1988a, b, 1989, 1995, 1998, 2001, 2004, 2005, 2007, 2011).

Dating

In the area of the Tsangpo bend in SE Tibet (Figure 1, left-hand side of Namcha Bawa), a last strong glacier advance is proved about or after 9.820+/−350 YBP. In addition, seven datings of trees from an 80 m high opening (1989) have been analyzed (Kuhle, 1998:83 Table 2: 99; 2004: 190 Figure 37). The eight ^{14}C-samples stem from the lower 32 m of the opening. These limnic basal sands, in which the trunks were embedded, have been overlain by 8 m thick varved clays. They provide evidence of an ice-dammed lake in this lower section of the Tsangpo valley at merely c. 3,000 m a.s.l. Accordingly, this ice-dammed lake is of the same age or younger than 48.580–9.820 YBP. Therefore, it is classified as being of the Last Glacial Maximum up to Late Glacial. The counting out of the varves yielded that the lake existed c. 1,000 years. It was situated between the ice complexes I2 and I3 (Figure 1, left-hand side of Namcha Bawa) and was dammed up by the Nyang Qu Glacier. The Nyang Qu Glacier, which was an outlet glacier of the ice complex I2, followed the Nyang Valley, reaching the Tsangpo Valley 17.5 km down-valley from the opening. Ground and lateral moraines confirm that the glacier bended into the Tsangpo Valley, and thus the ice-dammed lake came into being. These are several of the datings which establish an immediate genetic connection to the inland glaciation of Central Tibet and thus provide evidence of the Ice Sheet during the Last Glacial Period (LGP).

Discussion of datings

For several years, TCN-dating in High Asia has been carried out by some authors. However, a methodically fundamental mistake is that the astrophysical metric of cosmic radiation has not been sufficiently explored so far, and that the TCN-dating method therefore is not considered to be a reliable dating technique. In the critical remark (Kuhle and Kuhle, 2010), however, it is referred to the, at least up to now, unsolved astrophysical problem which states that one cannot assume constancy of cosmic radiation; the constancy assumption is, however, the indispensably

most important prerequisite for both TCN- and OSL-dating techniques.

As has been shown in other areas of the Himalaya, Karakoram, and Tibet, up to now, only ^{14}C-datings are glaciogeomorphologically safe, while the OSL- and TCN-datings carried out so far because of the high sea level are fourfold to tenfold overestimated, i.e., they led to too old ages. Thus, by means of ^{14}C-datings of moraines in the Khumbu Himal, a snowline (ELA)-depression up to 500 m has been evidenced during the Neoglacial period c. 2.1 and 4.2 ka ago; while the same ELA-depressions according to OSL- and TCN-ages were dated to c. 16–23 ka, i.e., they were overestimated by a factor 6.5. More OSL- and TCN-overestimations are evidenced for S- and Central Tibet and the Karakoram (Kuhle and Kuhle, 2010).

Probably the age of the TCN-data that so far have not been calibrated with regard to the high sea level of High Asia has been overestimated on the following grounds:

1. Obviously, the correction factors underestimate the amount of cosmic rays that really hit the surfaces of very high altitudes.
2. Due to magnetic field excursions, the amount of cosmic rays (CR) was additionally strengthened during the Late and High Glacial. This must have had a special effect at high altitudes, so that the age overestimation exponentially increases with moraine age.

This means that the Late Glacial moraine stages can already be extremely overestimated as to their age and thus differ from the Holocene stages in a clear age leap, while the glaciogeological findings do not confirm this great difference in age.

Actually there are already several independent proofs with regard to an "age leap" like this of the TCN-dating in High Asia (ibid. and Kuhle, 2011).

With regard to this deficiency of TCN-dating – that unfortunately has come into fashion – it is scientifically extremely important to take the complete glaciogeological and glaciogeomorphological setting into consideration and give to it the primary importance it deserves (Kuhle and Kuhle, 2010).

Summary

Since 1973, new data were obtained on the maximum extent of glaciation in High Asia. Evidence for an ice sheet covering Tibet during the Last Glacial Period means a radical rethinking about glaciation in the Northern Hemisphere. The ice sheet's subtropical latitude, vast size (2.4 million km²), and high elevation (6,000 m a.s.l.) are supposed to have resulted in a substantial, albedo-induced cooling of the Earth's atmosphere and the disruption of summer monsoon circulation. Moraines were found to reach down to 460 m a.s.l. on the southern flank of the Himalayas and to 2,300 m a.s.l. on the northern slope of the Tibetan Plateau, in the Qilian Shan region. On the northern slopes of the Karakoram, Aghil, and Kuen Lun mountains, moraines occur as far down as 1,900 m a.s.l. In southern Tibet, radiographic analyses of erratics suggest a former ice thickness of at least 1,200 m. Glacial polish and roches moutonnées in the Himalayas and Karakoram suggest former glaciers as thick as 1,200–2,700 m. On the basis of this evidence, an 1,100–1,600 m lower equilibrium line (ELA) has been reconstructed, resulting in an ice sheet of 2.4 million km², covering almost all of Tibet. ^{14}C ages classify this glaciation as MIS 3-2 in age (Würmian = Last Glacial Period (LGP), c. 60.000–18.000 years ago).

Bibliography

Anderson, D. M., and Prell, W. L., 1993. A 300 KYR record of upwelling off Oman during the late quaternary: evidence of the Asian southwest monsoon. *Paleoceanography*, **8**, 193–208.

Cline, R. (ed.), 1981. *Climap Project: Seasonal Reconstructions of the Earth's Surface at the Last Glacial Maximum*. New York: Geological Society of America, pp. 1–18.

COHMAP, 1988. Climatic changes of the last 18, 000 years: observations and model simulations. *Science*, **241**, 1043–1052.

Dainelli, G., and Marinelli, O., 1928. Le condizione fisiche attuali. Risultati Geologici e Geografici, Relazione scientifiche della Speditizione Italiana De Filippi nell'Himalaya, Caracorum e Turchestan Cinese (1913–1914), Ser.II, Vol. IV, Bologna.

Felzer, B., Webb, T., and Oglesby, R. J., 1998. The impact of ice sheets, CO², and orbital insolation on late quaternary climates: sensitivity experiments with a general circulation model. *Quaternary Science Reviews*, **17**, 507–534.

Gasse, F., Fontes, J Ch, Van Campo, E., and Wei, K., 1996. Holocene environmental changes in Bangong Co basin (Western Tibet). Part 4: Discussion and conclusions. *Palaeogeography, Palaeoclimatology, Palaeoecology*, **120**, 79–92.

Hewitt, K., 2009a. Catastrophic rock slope failures and late quaternary developments in the Naga Parbat – Haramosh Massif, Uper Indus basin, northern Pakistan. *Quaternary Science Reviews*, doi:10.1016/j.quascirev.2008.12019.

Hewitt, K., 2009b. Glacially conditioned rock-slope failures and disturbance-regime landscapes, Upper Indus Basin, northern Pakistan. *Geological Society, London, Special Publications*, **320**, 235–255, doi:10.1144/SP320.15.

Hsu, H., Zhang, C., and Wang, Y., 1998. Study on crustal movements of Tibetan plateau and its mechanism by geodetic methods. *"International Symposium on the Qinghai-Tibet Plateau"* 4, Xining, China.

Huntington, A., 1906. Pangong, a glacial lake in the Tibetan plateau. *Journal of Geology*, **14**, 599–617.

Kaufmann, G., and Lambeck, K., 1997. Implications of Late Pleistocene glaciation of the Tibetan plateau for present-day uplift rates and gravity anomalies. *Quaternary Research*, **48**, 267–279.

Kuhle, M., 1987. The problem of a Pleistocene Inland glaciation of the Northeastern Qinghai-Xizang-Plateau. In Hövermann, J., and Wenjing, W. (eds.), *Reports on the Northeastern Part of Quinghai-Xizang (Tibet)-Plateau by the Sino-German Scientific Expedition 1981*. Beijing: Science Press, pp. 250–315.

Kuhle, M., 1988a. Subtropical mountain- and highland-glaciation as ice age triggers and the waning of the glacial periods in the Pleistocene. *Chinese Translation Bulletin of Glaciology and Geocryology*, **5**(4), 1–17. in Chinese language.

Kuhle, M., 1988b. Zur Geomorphologie der nivalen und subnivalen Höhenstufe in der Karakorum-N-Abdachung zwischen Shaksgam-Tal und K2 Nordsporn: Die quartäre Vergletscherung und ihre geoökologische Konsequenz. In Becker, H. (ed.), *Tagungsbericht und wissenschaftliche Abhandlung des* 46. Deutschen Geographentag 1987 München. Steiner: Stuttgart, pp. 413–419.

Kuhle, M., 1989. Die Inlandvereisung Tibets als Basis einer in der Globalstrahlungsgeometrie fußenden, reliefspezifischen Eiszeittheorie. In *Petermanns Geographische Mitteilungen*. Justus Perthes Verlag: Gotha, Vol.133 (4), pp. 265–285.
Kuhle, M., 1995. Glacial isostatic uplift of tibet as a consequence of a former ice sheet. *GeoJournal*, **37**(4), 431–449.
Kuhle, M., 1998. Reconstruction of the 2.4 million qkm Late Pleistocene ice sheet on the Tibetan plateau and its impact on the global climate. *Quaternary International*, **45/46**, 71–108. Erratum: Vol. 47/48:173-182 (1998) included.
Kuhle, M., 2001. The Tibetan ice sheet; its impact on the palaeomonsoon and relation to the Earth's oribatal variations. *Polarforschung*, **71**(1/2), 1–13.
Kuhle, M., 2004. The high glacial (last ice age and LGM) ice cover in high and Central Asia. In Ehlers, J., Gibbard, P. L. (eds.), *Development in Quaternary Science*, 2c (Quaternary Glaciation – Extent and Chronology, Part III: South America, Asia, Africa, Australia, Antarctica), Amsterdam: Elsevier B.V, pp. 175–199.
Kuhle, M., 2005. Glacial geomorphology and ice ages in Tibet and surrounding mountains. *The Island Arc*, **14**(4), 346–367. Blackwell Publishing Asia Pty Ltd.
Kuhle, M., 2007. Critical approach to the methods of glacier reconstruction in High Asia (Qinghai-Xizang(Tibet) plateau, West Sichuan plateau, Himalaya, Karakorum, Pamir, Kuenlun, Tienshan) and discussion of the probability of a Qinghai-Xizang (Tibetan) inland ice. *Journal of Mountain Science (JMS)*, **4**(2), 91–123.
Kuhle, M., 2011. The High Glacial (LGP, LGM, MIS 3-2) southern outlet glaciers of the Tibetan inland ice through Mustang into the Thak Khola as further evidence of the Tibetan ice. *Journal of Nepal Geological Society*, submitted 14th November 2010.
Kuhle, M., and Kuhle, S., 2010. Review on dating methods: numerical dating in the quaternary of High Asia. *Journal of Mountain Science*, **7**, 105–122.
Kutzbach, J., Gallimore, R., Harrison, S., Behling, P., Selin, R., and Laarif, F., 1998. Climate and biome simulations for the past 21, 000 years. *Quaternary Science Reviews*, **17**, 473–506.
Marsiat, I., 1994. Simulation of the northern hemisphere continental ice sheets over the last glacial-interglacial cycle: experiments with a latitude-longitude vertically integrated ice sheet model coupled to a zonally averaged climate model. *Palaeoclimates*, **1**, 59–98.
Nesje, A., and Dahl, S., 2001. Glaciers and environmental change. Key Issues in *Environmental Change*: 1–200.
Norin, E., 1932. Quaternary climatic changes within the Tarim Basin. *Geographical Review*, **22**, 591–598. New York.
Oestreich, K., 1906. Die Täler des nordwestlichen Himalaya. *Petermanns Geographische Mitteilungen, Ergänzungsband*, **155**, 1–106.
Pachur, H.-J., and Wünnemann, B., 1995. Lake evolution in the Tengger desert, northwestern China, during the last 40, 000 years. *Quaternary Research*, **44**, 171–180.
Rutter, N., and Ding, Z., 1993. Paleoclimates and monsoon variations interpreted from micromorphogenic features of the Baoji Paleosols, China. *Quaternary Science Reviews*, **12**(10), 853–862.
Sirocko, F., Sarnthein, M., and Erlenkeuser, H., 1993. Century-scale events in monsoonal climate over the past 24, 000 years. *Nature*, **364**, 322–324.
Tafel, A., 1914. Meine Tibetreise. Eine Studienreise durch das nordwestliche China und durch die innere Mongolei in das östliche Tibet. 2 Bde., Karte, Stuttgart.
Trinkler, E., 1932. Geographische Forschungen in westlichen Zentralasien und Karakorum-Himalaya. *WissenschaftlicheErgebnisse der Dr. Trinklerschen Zentralasien-Expedition*. Berlin, pp. 1–133.
Verbitsky, M. Y., and Oglesby, R. J., 1992. The effect of atmospheric carbon dioxide concentration on continental glaciation of the northern hemisphere. *Journal of Geophysical Research*, **97**(D5), 5895–5909.
Wang, H., 2001. Effects of glacial isostatic adjustment since the late Pleistocene on the uplift of the Tibetan plateau. *Geophysical Journal International*, **144**, 448–458.
Wissmann, Hv., 1959. Die heutige Vergletscherung und Schneegrenze in Hochasien mit Hinweisen auf die Vergletscherung der letzten Eiszeit. *Akad Wiss Lit Abh Math-Natwiss Kl*, **14**, 1103–1407.
Xiao, J., Porter, S. C., An, Z., Kumai, H., and Yoshikawa, S., 1995. Grain size of quartz as an indicator of winter monsoon strength on the loess plateau of central China during the last 130, 000 yr. *Quaternary Research*, **43**, 22–29.
Yafeng, S., and Jing-Tai, W., 1979. The fluctuations of climate, glaciers and sea level since Late Pleistocene in China: Sea level, ice and climatic change. *Proceedings Canberra Symposium.* Canberra.
Yafeng, S., Binyuan, L., Jijun, L., Zhijiu, C., Benxing, Z., Qingsong, Z., Fubao, W., Shangzhe, Z., Zuhui, S., Keqin, J., and Jiancheng, K. (eds.), 1991. *Quaternary Glacial Distribution Map of Qinghai-Xizang (Tibet) Plateau, Scale 1:3, 000, 000*. Beijing: Science Press.
Zabirov, R. D., 1955. Oledenenie Pamira (Glaciations of the Pamir Mountains), Moscow, Geografgiz.

Cross-references

Climate Variability and High Altitude Temperature and Precipitation
Glacioisostasy
Himalaya
Ice Age
Ice Age Development Theory
Monsoonal Records Observed from Snow/Ice/Glacier
Quaternary Glaciation
Reconstruction of the Last Glaciations in the Whole of Asia
Sea-Level
Tibetan Plateau

LATENT HEAT OF CONDENSATION

Prem Datt
Research & Design Center (RDC), Snow and Avalanche Study Establishment, Himparishar, Chandigarh, India

The condensation is the opposite process of evaporation. Latent heat of condensation is energy released when water vapor condenses to form liquid droplets. The latent heat of condensation is defined as the heat released when one mole of the substance condenses. The temperature does not change during this process, so heat released goes directly into changing the state of the substance. It is expressed as kg/mol or kJ/kg. The energy released in this process is called heat of condensation. The heat of condensation of water is about 2,260 kJ/kg, which is equal to 40.8 kJ/mol. The heat of condensation is numerically exactly equal to the heat vaporization, but has the opposite sign. In the case of evaporation, the energy is absorbed by the substance, whereas in condensation heat is released by the substance. For example, as moist air is lifted and cooled, water vapor eventually condenses, which then allows for huge amounts of latent heat energy to be released, feeding the storm.

Bibliography

Armstrong, R. L., and Brun, E., 2008. *Snow and Climate: Physical Processes, Surface Energy Exchange and Modeling*. Cambridge: Cambridge University Press. ISBN 978-0-521-85454-2.
Jones, E. R., and Childers, R. L. *Contemporary College Physics.* Addison Wesley.
McClung, D., and Schaerer, P., 1993. *The Avalance Hand Book*. Seattle, WA: The Mountaineers.
The international classification for seasonal snow on the ground prepared by the ICSI-UCCS-IACS Working Group on Snow Classification, IHP-VII Technical Documents in Hydrology, IACS Contribution, UNESCO, Paris, 2009.

LATENT HEAT OF FUSION/FREEZING

Prem Datt
Research and Design Center (RDC), Snow and Avalanche Study Establishment, Himparishar, Chandigarh, India

Fusion is a physical process in which a solid converts into a liquid. The latent heat of fusion at a particular temperature is the amount of heat required to convert a unit mass of solid into liquid. For example, when ice melts into water the amount of heat required at 0°C is estimated equal to 334 kJ/kg, which is the latent heat of fusion of ice at 0°C. *This process is opposite to the process of freezing.* In a natural snowpack the fusion process generates melt-freeze polycrystals and melt-freeze clusters of the small rounded grains. A hard crust within snow results after multiple melt-freeze processes.

Bibliography

Armstrong, R. L., and Brun, E., 2008. *Snow and Climate: Physical Processes, Surface Energy Exchange and Modeling*. Cambridge: Cambridge University Press. ISBN 978-0-521-85454-2.
Jones, E. R., and Childers, R. L. *Contemporary College Physics.* Addison Wesley.
McClung, D., and Schaerer, P., 1993. *The Avalance Hand Book*. Seattle, WA: The Mountaineers.
The international classification for seasonal snow on the ground prepared by the ICSI-UCCS-IACS Working Group on Snow Classification, IHP-VII Technical Documents in Hydrology, IACS Contribution, UNESCO, Paris, 2009.

LATENT HEAT OF SUBLIMATION

Prem Datt
Research and Design Center (RDC), Snow & Avalanche Study Establishment, Himparishar, Chandigarh, India

Sublimation is a physical process in which a solid directly converts into a gaseous (vapor) state without going through a liquid state. The latent heat of sublimation at a particular temperature is the amount of heat required to convert a unit mass of solid into gas. For example, when ice sublimates into vapor, the amount of heat required at 0°C is estimated equal to 2,838 kJ/kg, which is the latent heat of sublimation of ice at 0°C. In the crystal growth of ice and snow in atmosphere, this process plays a dominant role. This process is opposite to the process of deposition.

Bibliography

Armstrong, R. L., and Brun, E., 2008. *Snow and Climate: Physical Processes, Surface Energy Exchange and Modeling*. Cambridge: Cambridge University Press. ISBN 978-0-521-85454-2.
Jones, E. R., and Childers, R. L. *Contemporary College Physics.* Addison Wesley.
McClung, D., and Schaerer, P., 1993. *The Avalance Hand Book*. Seattle, WA: The Mountaineers.
The international classification for seasonal snow on the ground prepared by the ICSI-UCCS-IACS Working Group on Snow Classification, IHP-VII Technical Documents in Hydrology, IACS Contribution, UNESCO, Paris, 2009.

LATENT HEAT OF VAPORIZATION/CONDENSATION

Prem Datt
Research and Design Center (RDC), Snow and Avalanche Study Establishment, Himparishar, Chandigarh, India

When a substance changes phase, the arrangement of its molecules changes, but its temperature does not change. If the new arrangement has a higher amount of thermal energy, then the substance absorbs thermal energy from its environment in order to make the phase change. If the new arrangement has a *lower* amount of thermal energy, the substance releases thermal energy to its environment.

Latent heat of vaporization is a physical property of a substance. It is defined as the heat required to change one mole of liquid at its boiling point under standard atmospheric pressure. It is expressed as kg/mol or kJ/kg. When a material in liquid state is given energy, it changes its phase from liquid to vapor; the energy absorbed in this process is called heat of vaporization. The heat of vaporization of water is about 2,260 kJ/kg, which is equal to 40.8 kJ/mol.

The vaporization is the opposite process of condensation. The heat of condensation is defined as the heat released when one mole of the substance condenses at its boiling point under standard pressure.

Bibliography

Armstrong, R. L., and Brun, E., 2008. *Snow and Climate: Physical Processes, Surface Energy Exchange and Modeling*. Cambridge: Cambridge University Press. ISBN 978-0-521-85454-2.
Jones, E. R., and Childers, R. L. *Contemporary College Physics.* Addison Wesley.
McClung, D., and Schaerer, P., 1993. *The Avalance Hand Book*. Seattle, WA: The Mountaineers.
The international classification for seasonal snow on the ground prepared by the ICSI-UCCS-IACS Working Group on Snow Classification, IHP-VII Technical Documents in Hydrology, IACS Contribution, UNESCO, Paris, 2009.

LATEROGLACIAL

Lasafam Iturrizaga
Geography/High Mountain Geomorphology, Institute of Göttingen, University of Göttingen, Göttingen, Germany

Synonyms

Ice-marginal

Definition

The term "lateroglacial" defines the ice-marginal areas along the lateral sides of the glacier. The lateroglacial environments grade downglacier into the latero-frontal and proglacial environments. They are composed of specific geomorphological and glaciological landform assemblages, such as ablation depressions, lateral moraines, breach lobes or earth pyramids. Lateroglacial landforms are mostly developed between the glacier and the adjacent valley flank in high mountain landscapes. However, they occur as well in the mountain forelands, especially along dam glaciers or outlet glaciers (e.g., in Iceland), but to a more limited extent. Relict lateroglacial sediments may serve as important geomorphological evidence for reconstructing the extent and ice thickness of former glaciations.

Bibliography

Iturrizaga, L., 2001. Lateroglacial valleys and landforms in the Karakoram Mountains (Pakistan). *GeoJournal*, **54**(2–4), 397–428. Tibet and high Asia (VI), Glacio-geomorphology and prehistoric glaciation in the Karakorum and Himalaya.

Iturrizaga, L., 2003. The distribution and genesis of lateroglacial valleys in the Karakoram Mountains (Pakistan). *Zeitschrift für Geomorphologie N.F.*, **130**(Suppl. Bd), 51–74.

Cross-references

Ablation Depression
Lateroglacial Landform Systems

LATEROGLACIAL LANDFORM SYSTEMS

Lasafam Iturrizaga
Geography/High Mountain Geomorphology, Institute of Göttingen, University of Göttingen, Göttingen, Germany

Synonyms

Ice-marginal landforms

Definition

Lateroglacial landforms are located at the lateral margins of the glaciers and belong to the glacial landscape systems. Down glacier they pass over into the laterofrontal and proglacial sediment environments. Lateroglacial landforms show characteristic landform sequences and assemblages (i.e., lateroglacial valleys, ablation depressions, earth pyramids) and are classified as a specific geomorphologic unit of the glacial environment.

Distribution

Lateroglacial landforms may occur at any glacier, preferentially at valley glaciers in mountain regions with sufficient debris supply areas and their associated forelands (i.e., in the European Alps, the Andes, and the Himalayas). They are best developed in the Karakoram Mountains (72°–79°E; 35°–36°N), where they have been investigated systematically as a specific geomorphological unit along 53 glaciers in regard to their distribution, evolution, and morphodynamics (Iturrizaga, 2001, 2003, 2007). The Karakoram shows the highest concentration of large valley glaciers outside of the polar regions with glacier lengths of up to 72 km. In combination with a surrounding high mountain relief of over 8,000 m, the Karakoram provides large-sized debris supply areas for the formation of a heterogeneous lateroglacial environment. Lateroglacial sediment complexes may attain a length of up to several to tens of kilometers and can be referred to as lateroglacial valleys. Besides their large horizontal distribution, they are spread over a considerable vertical range in the Karakoram and occur between altitudes of about 2,500–5,000 m. The upper limit of lateroglacial sediments deriving from the glacier is theoretically given by the altitude of the snow line. Due to the fact that a major part of the glaciers are avalanche-fed glaciers and therefore show steep inclined head walls of up to 3,000 m in absolute height, the distribution of lateroglacial sediments starts usually 1,000–1,500 m lower than the snow line.

Types of lateroglacial landforms and their processes of formation

The transition from the valley flank to the glacier emerges in different morphological variations. One of the most well-known and prominent landforms are the lateroglacial valleys, which are ice-marginal depressions between the glacier and the valley flank and may be filled with sediments. They even show in some cases an own drainage system over short distances. They are not true valleys in sensu stricto, but rather glacier-marginal discontinuous depressions. Where mountain spurs stand out against the glaciated main valley, the lateroglacial valleys may be interrupted. The topographical depression can be filled up with a wide range of different types of sediments or the sediments themselves may even be the trigger for the formation of the lateroglacial valleys. One of the main characteristics of the lateroglacial sediment regime is the damming effect by the glacier, which results in a large-scaled sediment storage along the glacier margins. The lateroglacial sediments are highly polygenetic landforms.

A characteristic type of lateroglacial valleys is the *lateral moraine valley*. It is a mostly linear depression or sediment assemblage between the lateral moraine and the valley flank (Oestreich, 1906). It had been erroneously often referred to as "*ablation valley*." Visser (1938) carried

out the first systematic investigation on these landforms and postulated an insolation-controlled distribution of all lateroglacial landforms. This terminology has been widely criticized by many authors (v. Klebelsberg, 1938; Hewitt, 1993) as the lateroglacial depressions show various formation processes. Consequently, the nongenetical expression "lateroglacial valleys" has been introduced (Iturrizaga, 2001). However, the formation of a lateroglacial valley might be triggered by the presence of an ablation depression as it can provide initial sediment traps.

The formation of lateral moraine valleys is mainly a result of (a) dumping processes of the lateral moraine against the valley flank, especially during times of a comparatively smaller extent of the glacier, and (b) different type of debris inputs from the adjacent tributary valleys and valley slopes. Their width attains a size of up to 1 km. The great dimension already indicates that ablation processes only play a subordinated role in their formation. The *lateral moraine* is the most distinct depositional landform in lateroglacial environments. It may attain a height of about 250 m. Its large size has been attributed to repetitive glacier advances and accordingly to various deposition processes. The lateral moraine is often composed of an older moraine core, which has been superimposed by younger moraine layers and/or processes of moraine accretion. The time period of their formation goes in general back to the Neoglacial and Little Ice Age. Once the lateral moraine has been built up, it prevents the direct debris transfer from the glacier to the interior of the lateroglacial valleys. Consequently, the sedimentary system in the lateroglacial depression is well protected from glacial activities, unless some overspilling or breakthrough of the lateral moraine takes place. The lateral moraine also impedes the drainage of the tributary rivers into the glacier system.

The lateral moraine valleys are distinguished into two principal types: (a) The V-shaped lateral moraine valley, in which the lateral moraine is directly connected with the adjacent valley flank. Its origin goes mainly back to dumping processes occurring at the glacier margin (Figure 1). (b) The lateral moraine valley with a valley bottom floor (Figure 2). The incorporated sediments are composed of heterogeneous debris sources (Figure 3):

1. Primary processes of rock disintegration such as ice avalanches and freeze-thaw processes as well as glaciofluvial sediments from the main and tributary glaciers provide debris for the formation of lateroglacial sediments, especially for the formation of the lateral moraine.
2. A considerable part of the debris supply for the lateroglacial sediment complexes derives from the tributary valleys, in particular at glaciers framed by highly dissected mountain relief (Figure 1). The sediment cones, such as alluvial fans, debris flow cones, and avalanche cones, drain toward the glacier either into an existent ice-marginal depression or even onto the glacier. Especially large-sized, catastrophic debris flows can even initiate the formation of a lateroglacial valley. Rockslides, debris flows, and snow avalanches deposited into a lateroglacial valley frequently dam lateroglacial rivers and cause the deposition of lacustrine sediments. As a result, a considerable proportion of the lateroglacial sediments is of non-glacial origin. This fact has to be taken into consideration regarding glacier reconstruction in recent non-glaciated

Lateroglacial Landform Systems, Figure 1 V-shaped lateral moraine valley at the Pumari Chhish glacier in 4,100 m. Photo: L. Iturrizaga (1999).

Lateroglacial Landform Systems, Figure 2 Lateral moraine valley (◊) at the almost 2 km broad Batura glacier in S-aspect. Debris supply derives mainly from the tributary valleys (←) and the resedimentation of slope moraines (Δ). In the background the Batura massiv (7,885 m) is visible. Photo: L. Iturrizaga (2000).

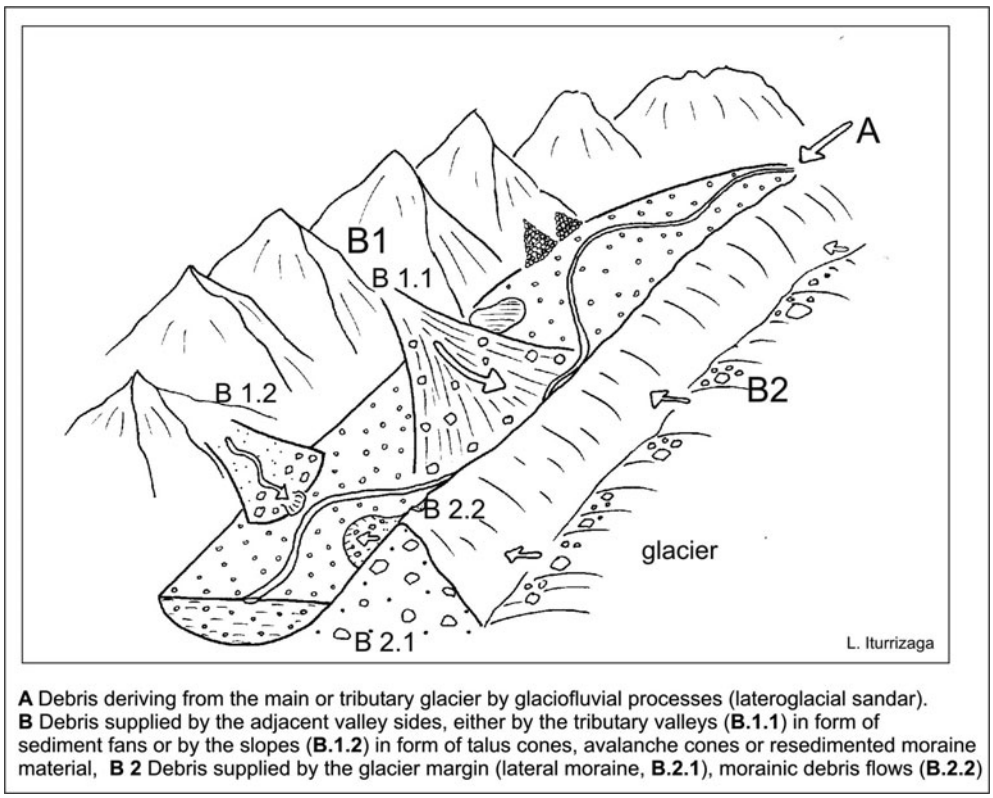

A Debris deriving from the main or tributary glacier by glaciofluvial processes (lateroglacial sandar).
B Debris supplied by the adjacent valley sides, either by the tributary valleys (**B.1.1**) in form of sediment fans or by the slopes (**B.1.2**) in form of talus cones, avalanche cones or resedimented moraine material, **B 2** Debris supplied by the glacier margin (lateral moraine, **B.2.1**), morainic debris flows (**B.2.2**)

Lateroglacial Landform Systems, Figure 3 Source areas of debris supply for lateroglacial valleys.

mountain valleys. Dendritic glaciers in which the individual tributary glaciers recede and loose the contact to the main glacier are prone to the formation of lateroglacial sediment complexes.

3. The lateroglacial sediment landscape is built up to a great extent by the secondary debris supply in form of the reworking of older glacigenic deposits mantling the valley flanks (Figure 4). Many glaciers show a close interfingering of Late Glacial slope moraines and younger lateroglacial landforms. After the gradual down-melting of the Pleistocene glacier surface, moraine deposits remain along the lateroglacial margins, partly as terraces, partly as amorphous deposits and are dislocated into the lateroglacial valley by different types of mass movements.
4. In some parts, the sediments are deposited in the form of small-scaled *lateroglacial sandar*. These are glaciofluvial deposits which originate directly from the melt waters of the main or the tributary glacier. They are located between the glacier and the valley flank or the lateral moraine. After the deglaciation, these sediments are preserved as kame terraces.

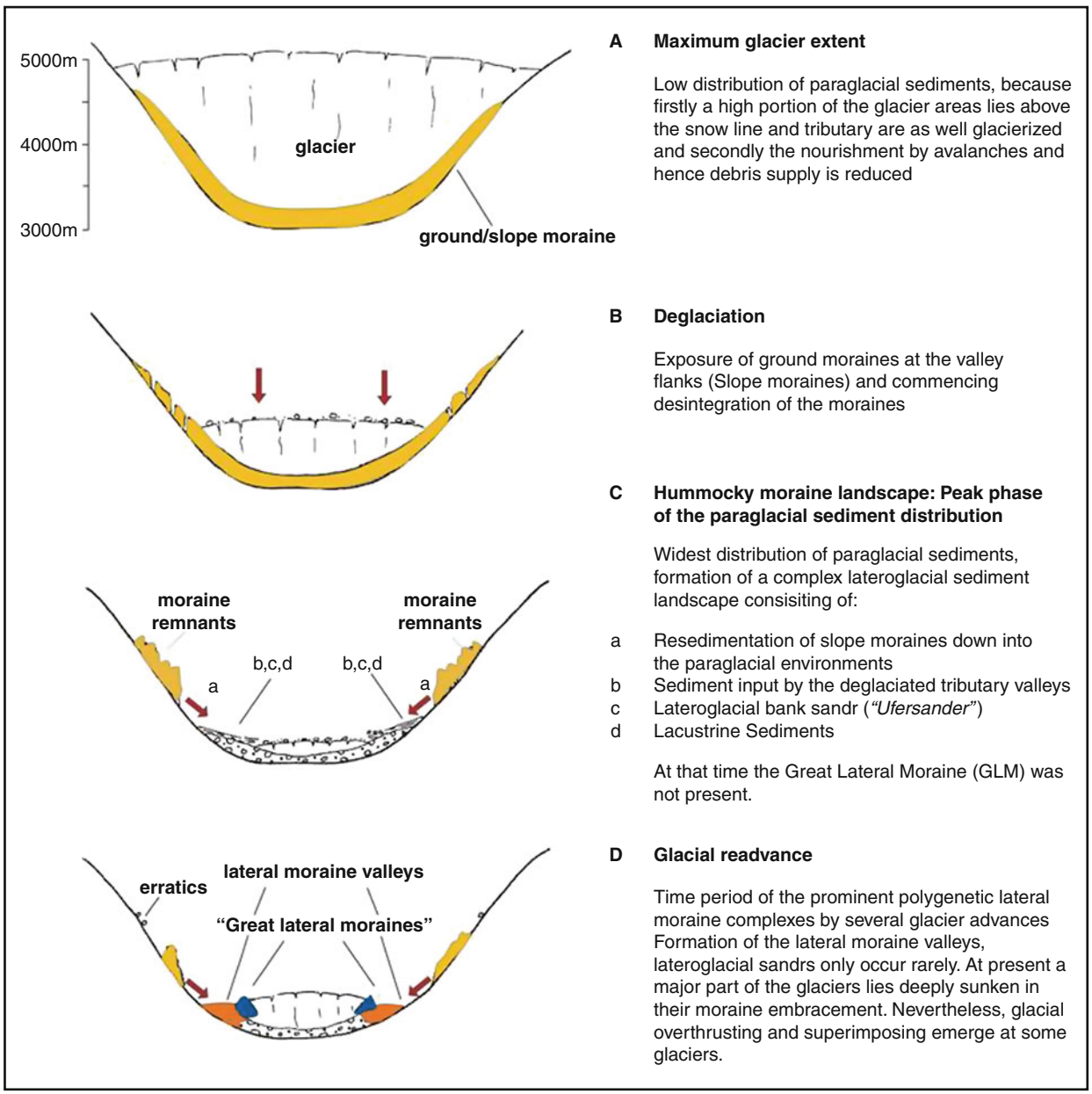

L. Iturrizaga

Lateroglacial Landform Systems, Figure 4 Genesis of the lateroglacial valleys deduced from the glacial history.

Relict lateroglacial valleys occur as high as 1,000 m above the present glacier surfaces and are important landforms for reconstructing the Pleistocene glacier thickness.

Summary

Lateroglacial landforms are composed of a large variety of different sediment types. The higher and more spaciously the surrounding mountain relief of the glacier in general is, the more complex are the lateroglacial landform systems. In many mountain areas, i.e., the European Alps, the Canadian Rocky Mountains, and also the Himalayas, lateral moraine valleys represent rather stable landforms. However, at many locations, they are in the stage of destruction due to glacier surface lowering and the missing abutment of the glacier. In the Karakoram, lateral moraine valleys may also be destroyed by present glacier advances or lateral widening as those glaciers are even today highly dynamic in the form of short-term glacier advances or surges. Lateroglacial valleys are a major location for temporary settlements and their pasture areas. Changes in the settlement situation are valuable indicators for glacier dynamics along the lateroglacial margins.

Bibliography

Hewitt, K., 1993. Altitudinal oranization of Karakoram geomorphic processes and depositional environments. In Shroder, J. F., jr (ed.), *Himalaya to the Sea. Geology, Geomorphology and the Quaternary.* London: Routledge, pp. 159–183.

Iturrizaga, L., 1999. Typical debris accumulation forms and formations in High Asia. A glacial-history-based concept of the origin of postglacial debris accumulation landscapes in subtropical high mountains with selected examples from the Hindu Kush, the Karakoram and the Himalayas. In Kuhle, M. (ed.), Tibet and High Asia (V), *GeoJournal*, **47**(1–2), 277–339.

Iturrizaga, L., 2001. Lateroglacial valleys and landforms in the Karakoram mountains (Pakistan). In Kuhle, M. (ed.), Tibet and High Asia (VI), Special Volume, *GeoJournal*, **54**(2–4), 397–428.

Iturrizaga, L., 2003. The distribution and genesis of lateroglacial valleys in the Karakoram mountains (Pakistan). *Zeitschrift für Geomorphologie N.F*, **130**, 51–74.

Iturrizaga, L., 2007. Die Eisrandtäler im Karakorum: Verbreitung, Genese und Morphodynamik des lateroglazialen Sedimentformenschatzes. In *Geography International*. Aachen: Shaker Verlag, Vol. 2, p. 389.

Iturrizaga, L., 2008. Post-sedimentary transformation of lateral moraines: the tributary tongue basins of the Kvíárjökull (Iceland). *Journal of Mountain Sciences*, **5**(1), 1–16.

Oestreich, K., 1906. Die Täler des nordwestlichen Himalaya. In *Petermanns Geographische Mitteilungen*, Vol. 155, 106 pp.

Visser, P. C., 1938. Glaziologie. In Visser, Ph. C., and Visser-Hooft, J. (eds.) Wissenschaftliche Ergebnisse der Niederländischen Expeditionen in den Karakorum und die angrenzenden Gebiete in den Jahren 1922, 1925 und 1929/30. vol. 2, 215 pp.

von Klebelsberg, R., 1938. Visser's Karakorum-Glaziologie. *Zeitschrift für Gletscherkunde*, **26**(3/4), 307–320.

Cross-references

Ice-Marginal Deposition
Ice-Marginal Processes

LAURENTIDE ICE SHEET

John T. Andrews
Institute of Arctic and Alpine Research and Department of Geological Sciences, University of Colorado, Boulder, CO, USA

Definition

Laurentide Ice Sheet (LIS) – refers to an Antarctic-size ice sheets that extended from the general area of the Great Lakes in the USA northward to the Canadian Arctic coast, and westward from the uplands and fjords of Baffin Island and Labrador to the foot of the Rocky Mountains (Figure 1). In the west, it was at times contiguous with the Cordilleran Ice Sheet, and in the NE merged with the Innuitian Ice Sheet.

Introduction

The LIS had an area of approximately 12×10^6 km^2, a central thickness estimated to be in the range of 3–4 km, and sufficient mass to cause a worldwide fall in sea level of around 70± m, out of a total global sea level extraction of ~120–130 m due to expansion of ice sheets and glaciers worldwide (Figure 2). The term LIS should strictly be only applied to the last great ice sheet of the Wisconsinian Glaciation (Figure 2), but it is frequently used to cover a broader span of Quaternary time. Because of its area, height, and volume the LIS has to be considered a major component in the late Quaternary climate of our planet, seriously influencing ice sheet/ocean/atmospheric interactions. Waters from the ice sheet debouched into three marine basins – drainage from the Great Lakes westward were directed into the Gulf of Mexico, waters from the long eastern margin entered Baffin Bay, the Labrador Sea and the western North Atlantic, whereas the northern margin drained to the Arctic Ocean (Figure 1). The input of meltwater into the oceans has been called upon as having a significant impact of the thermohaline circulation of the oceans. Tidewater outlets and ice streams also injected icebergs into the North Atlantic and Arctic oceans. Ice-rafted debris (IRD) from the North American continent has been traced across the Arctic Ocean and in the North Atlantic as far east as the Portugal margin.

A brief history of concepts about the LIS

By the 1890s, a good deal of research had been carried out in the glaciated area of the USA and in southern Canada. In 1898, Tyrrell produced a map of the former North America ice sheets. This map is remarkably similar in many ways to present-day concepts of the LIS, that is, an ice sheet that like the Antarctic Ice Sheet, had several dispersal center with ice divides over Labrador, Foxe Basin, Keewatin, and the Patrician Center off SW Hudson Bay. This notion prevailed until the 1940s when Flint argued for the growth of an ice sheet from the mountains of the eastern Canadian Arctic to finally form a massive

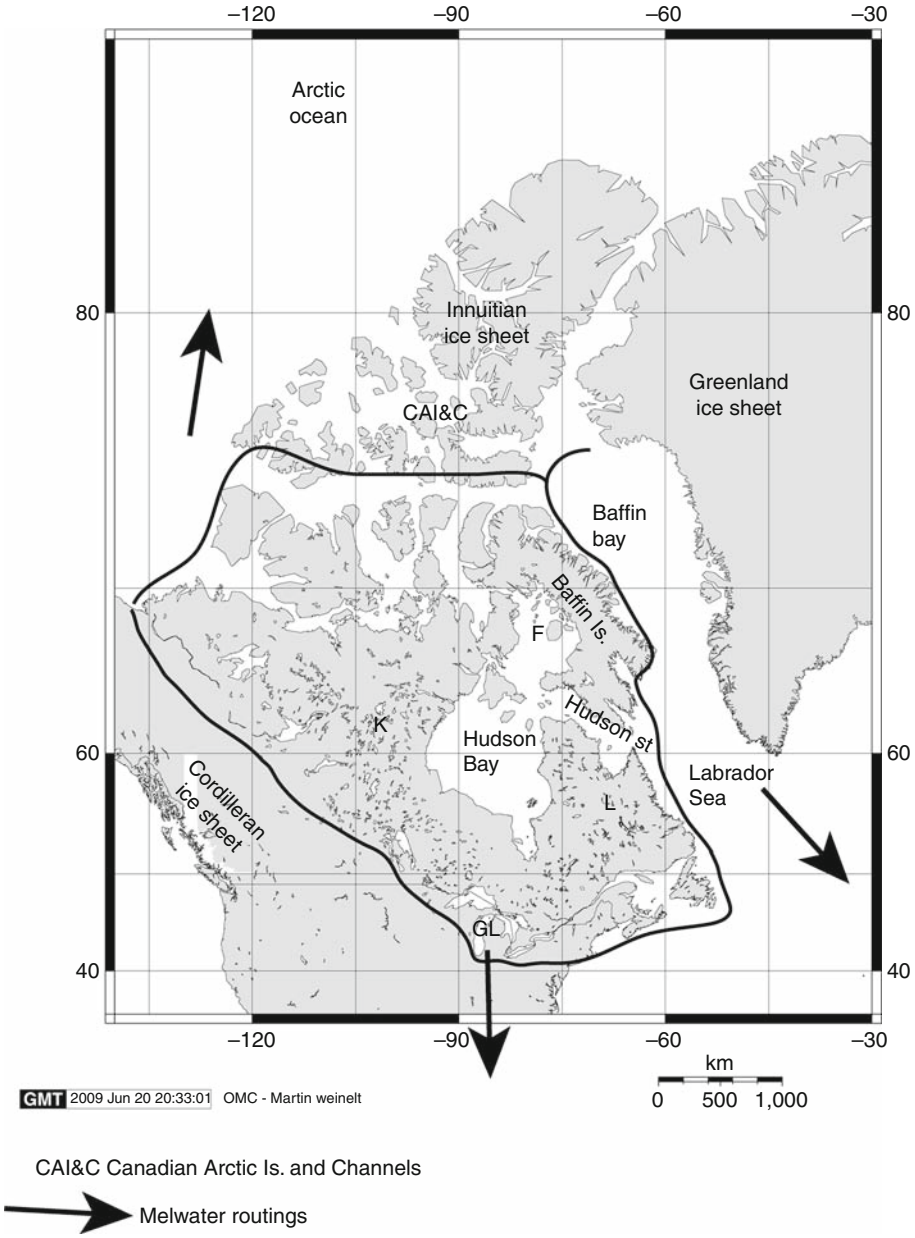

Laurentide Ice Sheet, Figure 1 North American showing the outline of the Laurentide Ice Sheet during the last glacial maximum. K = Keewatin ice divide, L = Labrador ice divide, F = Foxe Basin ice divide.

single-domed ice sheet centered over Hudson Bay. Flint's model was based on a conceptual model for the growth and development of the ice sheet. This model continued to have adherents into the 1970s and 1980s but is now largely abandoned.

Wide-ranging field observations in the Eastern Canadian Arctic in the late 1950s and 1960s, combined with adequate topographic maps, aerial photographs, satellite imagery, and increased knowledge of the tectonic evolution of the North Atlantic region during the Tertiary, resulted in an appreciation of the role that the high rolling uplands of the Eastern Canadian Arctic played in the onset of glaciation, and in the overall complex pattern of shifts in flow regimes during the Wisconsinian Glaciation.

Onset of glaciation

Our knowledge of the growth and buildup of the LIS during the interstadials of marine isotope stage (MIS) 5, namely 5d and 5b, is limited (Figure 2). The last full interglacial over North America (MIS 5e) was warmer than present, and it is possible that many of the smaller ice caps

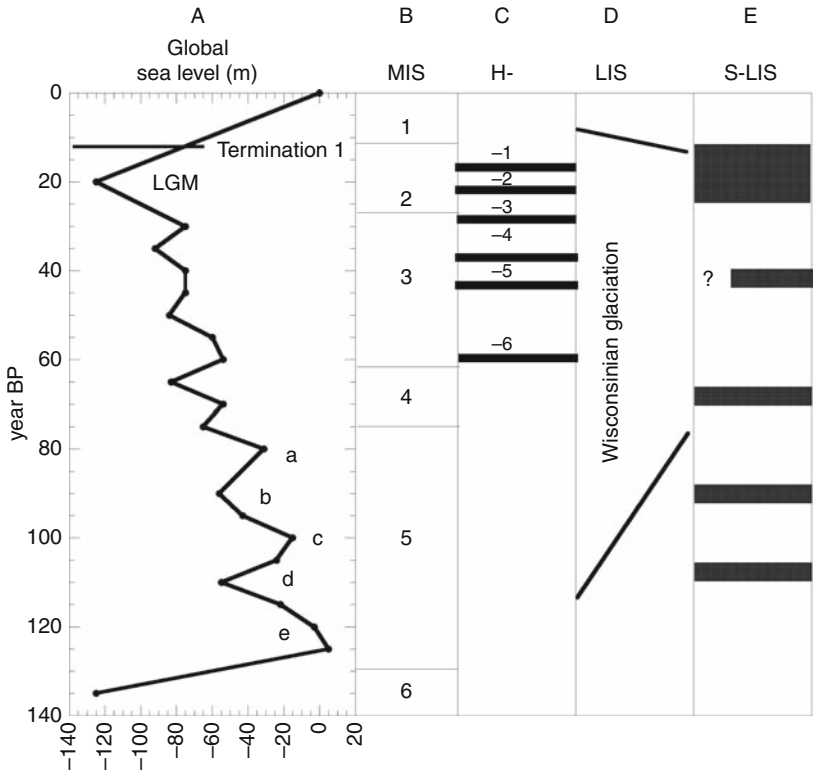

Laurentide Ice Sheet, Figure 2 Evolution of global sea level during the last glacial (Wisconsinian) cycle. (**a**) global sea level (Shackleton 1987); (**b**) marine isotope stages (MIS); (**c**) Heinrich (H-) events; (**d**) age span of the Wisconsinian Glaciation; (**e**) glacial episodes of the Laurentide Ice Sheet (LIS) in the area of the Great Lakes (Figure 1) (Karrow et al., 2000).

and glaciers in the Eastern Canadian Arctic disappeared. On the global level, the relationship between ice volume and $\delta^{18}O$ of marine foraminifera indicate that the growth of ice sheets during MIS 5d was remarkably rapid as global sea level fell to –55 m in ~10,000 years. What fraction of this global extraction of water for ice sheet buildup is associated with the LIS is largely unknown, but on general climatic grounds it seems reasonable that a considerable fraction of the 55 m of global sea level was locked into the initial growth of the LIS.

The global pattern of changes in sea level, a proxy for ice sheet growth and decay, has been successfully linked to changes in insolation, which in turn has been linked to the orbital variations of the Earth relative to the Sun – the so-called Milankovitch orbital variations. Spectral analysis of $\delta^{18}O$ time series covering the last 700,000 years shows that the variations in sea level, hence ice sheet mass, have 100,000, 41,000, and 25,000 periodicities, and this gives an initial template for evaluating the history of the LIS. However, subsequent research has shown that the LIS is also marked by much shorter periodic events, such as Heinrich (H-) events (Figure 2).

The uplands of the Eastern Canadian Arctic, that is the largely undissected Precambrian shield that lies to the west of the Tertiary rift-margin along the Labrador and Baffin Island coast, have a large fraction of their elevation >500 m asl. Imagery and fieldwork indicate that during the Little Ice Age (LIA) ca. AD 1400–2000 large fraction of these uplands were covered with permanent snow beds or small ice caps, thus demonstrating the sensitivity of these areas to relatively small changes in net mass balance. Hence, virtually all attempts to model the development and growth of the LIS over the last 120,000 years, show the initial growth of the ice sheet over the uplands of Labrador and Baffin Island. As conditions cooled, it is also probable that ice sheets developed over the somewhat lower plateaus terrain of Keewatin, west of Hudson Bay, and an ice sheet may have developed across the High Canadian Arctic islands and Channels. Thus, the initial movement of the various accumulation centers would have been from the uplands through the fiords of Labrador and Baffin Island, and toward the large interior seas of Hudson Bay and Foxe Basin. A critical question is whether the advancing ice sheets based over Labrador and Baffin Island merged across Hudson Strait prior to glacial inundation of Hudson Bay – if that did not happen then a large glacially dammed lake would have been ponded within the Bay.

At some point, possibly in MIS 4, Hudson Bay, and Foxe Basin were filled and the LIS then became a marine-based ice sheet, somewhat similar in that respect

to the West Antarctic Ice Sheet today. Because of the mass of the LIS the bedrock under the ice sheet would be isostatically depressed – thus meaning a large fraction of the ice sheet was grounded below the sea level, and linked to the North Atlantic via the deep graben of Hudson Strait (Figure 1). Hudson Bay, Foxe Basin, and Hudson Strait are floored with Paleozoic carbonates composed of calcite and dolomite, and these rocks provide powerful tracers of ice sheet activity in the adjoining deep-sea basins of the Labrador Sea and Baffin Bay.

Glacial landscapes

The extension of the LIS along its eastern margin is limited by the presence of the adjacent ocean basins, and it is in these areas that some trace of the history of the ice sheet can be recovered in piston cores through marine sediments. The deep water connections between the ice sheet (~450 m at the Hudson Strait sill, without isostatic depression) and the Labrador Sea represent one major potential point of instability; others exist in other deep marine embayments, such as the Gulf of St Lawrence. However, on the grand scale of the LIS there is also another large spatial difference, that is between the "hard bed," glaciological speaking, of the sediments produced by erosion of the Precambrian granites and gneisses, versus the "soft-bed" younger sedimentary rocks that flank the shield rocks along the southern flank. Reconstruction of profiles of the ice sheet and its outlets in the areas of the Canadian Prairies, Iowa, and in the Great Lakes indicate that the basal shear stress was much lower and the ice much thinner than where the ice sheet was moving across the shield bedrock. Thus the configuration of the LIS and its potential response to climate and other changes are quite different from the neighboring Greenland Ice Sheet.

The effect of the combination of bedrock, elevation, and tectonics on the large-scale patterns of glacial erosion is evident on satellite imagery. The uplifted eastern rim of the Shield is dissected by fiords, and large-scale grabens extend into or toward the center of the ice sheet. On the flanks of Foxe Basin and Hudson Bay where the eastward flowing ice attained thicknesses of 2 km or more the Shield rocks have been glacially eroded along joint and fracture planes to form a landscape of glacial scour, with limited thickness of glacially derived sediments (till). Between the fiord landscape and the scoured areas there is frequently an area (usually >400 m asl) with little or no scour; this is interpreted as an area that was covered by thinner ice with basal temperatures below the pressure melting point (i.e., cold-based ice). In the flanking region along the southern margin of the ice sheet the thickness of till is greater and the underlying bedrock is masked by glacial and glaciofluvial sediments. Contrary to some theories, the area at the geographic center of the LIS, the western Hudson Bay lowlands, has a thick sequence of preserved non-glacial and glacial sediments that are a critical record of the LIS.

The LIS and Wisconsinian glaciation

The marine isotope records form a template for global changes in ice sheet volumes acting on multi-millenial scales (Figure 2). How far does the stratigraphic record from the area of the LIS match this master template, indeed how far can we express the history of the LIS in a single description versus regional differences in glacial history? This question faces several major problems. First is the fact that the stratigraphic record within the margins of the LIS is largely an intermittent record of temporal events at the best; in addition, the ice sheet has also the potential to erode evidence of past oscillations. Secondly, to place the history of the LIS into a time perspective to match with the $\delta^{18}O$ record requires (a) materials that can be dated, and (b) dating methods that span, ideally, 120,000 years or so. It should be noted that the marine time series are not without problems, in-so-far-as the main "absolute" dating method is radiocarbon dating of foraminifera, which only extends back 40,000–50,000 years BP. Thus, the chronology for MIS 4 and 5 is largely derived from a process of correlation with the astronomical (insolation) variations with links to U-series dates on raised coral reefs. Within or at the margins of the LIS implications for ice sheet growth or retreat are based on the stratigraphic sequence (including the nature of the sediments and paleobiological data) with ^{14}C dates being derived from wood, peat, shells, whalebone, or other organic materials. Often exposed sections have no material for dating or events are dated at >40,000 BP. In the last 10–20 years, a dating revolution has occurred with the advent of cosmogenic exposure age dating. This method allows, for the first time, moraines and eroded surfaces to be directly dated. This approach has shed new light on the LIS history, especially in Arctic areas, where materials for ^{14}C dating were scarce or absent, but where large surface boulders and exposed bedrock are abundant.

The LIS probably grew from its inception grounds during the interglacials of MIS 5 and expanded across the Gulf of St. Lawrence and into the Great Lakes during MIS 4 ca. 75,000 years ago (Figure 2). The history of the ice sheet during MIS 3 is proving difficult to unravel but the ice sheet may have been largely confined to the "hard bed" of the PreCambrian shield. Whether the glaciologically sensitive area of the interior basin of Hudson Bay was ever deglaciated is debatable and hinges on issues involved with dating marine sediments in the Hudson Bay lowlands and the interpretation of sediments in the Labrador Sea.

Heinrich events and LIS instability

The relatively smooth intervals of growth and retreat of ice sheets that are implied in the ocean ^{18}O records were infact punctuated by massive instabilities of the marine-based LIS. Heinrich (H-) events (Figure 2) record massive outbreaks of meltwater and icebergs into the North Atlantic, with the major source being the ice

stream in Hudson Strait. H-events have been documented in the Labrador Sea eastward toward Europe due to their distinctive mineralogical composition, mainly detrital carbonate (DC) grains. Similar, but temporally offset DC events occur in Baffin Bay, representing collapse of the LIS and Innuitian ice sheets across the Canadian Arctic channels that lead into Baffin Bay. Detrital carbonate events also occur in Arctic Ocean sediments and represent events along the Arctic margin of the LIS and Innutian ice sheets. The massive thickness of DC sediments associated with H-4 in the Labrador Sea argues that Hudson Bay was not ice-free during MIS 3.

The last glacial maximum (LGM) and deglaciation of the LIS

The LIS expanded from its more restricted, more largely unmapped, extent during MIS3 to reach its maximum last glacial extent ~20,000 years BP (Figure 1). Note that the LGM is also marked by a major H-event (Figure 2). Given the geographic and climatic extent of the LIS during the LGM, it is unlikely that every margin of the ice sheet reached its maximum extent at exactly the same time. Indeed, for much of the eastern flank of the ice sheet the exact location of the margin at ~20,000 years BP is unknown and does not appear to be marked by large moraine systems, possibly because the ice sheet was cold-based.

The deglaciation of the LIS has now been mapped and dated across thousands of sites. Viewed in the light of the previous 120,000 years the deglaciation is relatively abrupt and is termed, globally, Termination I (Figure 2). Briefly the LIS retreats asymmetrically with initial high rates of ice retreat along the southern and western margins, with little change along the long eastern margin. As summer insolation increased, meltwaters were directed into adjacent oceans (Figure 1). The stability of the ice sheet was weakened by a massive collapse through Hudson Strait during H-1 (16,000 years ago). As the ice sheet retreated in the south and west at some point the continental drainage divide was revealed and a series of large, glacially dammed lakes were formed – these lakes are often lumped under the name Glacial Lake Agassiz. The final demise of much of the LIS occurred ca 8.4 years ago when waters from the Labrador Sea, penetrating through Hudson Strait, breached the remaining ice over Hudson Bay and connected with and drained glacial lakes that had been dammed south of the ice sheet. This outburst event and earlier meltwater events impacted the thermohaline circulation.

In subsequent years, the ice retreated and disappeared from the Labrador plateaus but the last remnants of the LIS still exist across central Baffin Island in the form of the Barnes Ice Cap.

Summary

The Laurentide Ice Sheet was the largest ice sheet in the Northern Hemisphere, comparable in size to the present Antarctic Ice Sheet. Growth and retreat were controlled by periodic changes in insolation but its marine-based nature made it susceptible to major collapses with massive outflows of meltwater and icebergs.

Bibliography

Andrews, J. T., 1998. Abrupt changes (Heinrich events) in late Quaternary North Atlantic marine envrionments: a history and review of data and concepts. *Journal of Quaternary Science*, **13**, 3–16.

Andrews, J. T., Kirby, M. E., Aksu, A., Barber, D. C., and Meese, D., 1998. Late Quaternary Detrital Carbonate (DC-) events in Baffin Bay (67°–74° N): Do they correlate with and contribute to Heinrich Events in the North Atlantic? *Quaternary Science Reviews*, **17**, 1125–1137.

Briner, J. P., Miller, G. H., Davis, P. T., Bierman, P. R., and Cafee, M., 2003. Last Glacial Maximum ice sheet dynamics in Arctic Canada inferred from young erratics perched on ancient tors. *Quaternary Science Reviews*, **22**, 437–444.

Clark, P. U., and Walder, J. S., 1994. Subglacial drainage, eskers, and deforming beds beneath the Laurentide and Eurasian ice sheets. *Geological Society of America Bulletin*, **106**, 304–314.

Clark, P. U., Licciardi, J. M., MacAyeal, D. R., and Jenson, J. W., 1996. Numerical reconstruction of a soft-bedded Laurentide Ice Sheet during the last glacial maximum. *Geology*, **24**, 679–682.

Denton, G. H., and Hughes, T. J., 1981. *The Last Great Ice Sheets*. New York: Wiley, p. 484.

Dyke, A. S., 2004. An outline of North American deglaciation with emphasis on central and northern Canada. In *Quaternary Glaciations – Extent and Chronology*, Part II. New York: Elsevier, pp. 373–424.

Dyke, A. S., Andrews, J. T., Clark, P. U., England, J. H., Miller, G. H., Shaw, J., and Veillette, J. J., 2002. The Laurentide and Innuitian ice sheets during the Last Glacial Maximum. *Quaternary Science Reviews*, **21**, 9–31.

Fulton, R. J. (ed.), 1989. *Quaternary Geology of Canada and Greenland*, Geological Survey of Canada, Geology of Canada No. 1, Queens Printer, Ottawa, 839 pp.

Hesse, R., Klaucke, I., Ryan, W. B. F., et al., 1997. Ice-sheet sourced juxtaposed turbidites systems in labrador sea. *Geoscience Canada*, **24**, 3–12.

Karrow, P. F., Dreimanis, A., and Barnett, P. J., 2000. A proposed diachronic revision of Late Quaternary time-stratigraphic classicagtion in the Easterrn and Northern Great Lakes area. *Quaternary Research*, **54**, 1–12.

Marshall, S. J., and Clarke, G. K. C., 1999. Ice sheet inception: subgrid hypsometric parameterization of mass balance in an ice sheet model. *Climate Dynamics*, **15**, 533–550.

Marshall, S. J., Teller, J. S., and Clarke, G. K. C., 2002. North American ice sheet reconstructions at the Last Glacial Maximum. *Quaternary Science Reviews*, **21**, 175–192.

Matthews, W. H., 1974. Surface profiles of the Laurentide Ice Sheet in its marginal areas. *Journal of Glaciology*, **13**, 37–43.

Miller, G. H., Wolfe, A. P., Steig, E. J., Sauer, P. E., Kaplan, M. R., and Briner, J. P., 2002. The Goldilocks dilemma: big ice, little ice, or "just-right" ice in the Eastern Canadian Arctic. *Quaternary Science Reviews*, **21**, 33–48.

Shackleton, N. J., 1987. Oxygen isotopes, ice volume and sea level. *Quaternary Science Reviews*, **6**, 183–190.

Stokes, C. R., Clark, C. D., Darby, D. A., and Hodgson, D. A., 2005. Late Pleistocene ice export events into the Arctic Ocean from the M'Clure Strait Ice Stream, Canadian Arctic Archipelago. *Global and Planetary Change*, **49**, 139–162.

Sugden, D. E., 1977. Reconstruction of the morphology, dynamics and thermal characteristics of the Laurentide Ice Sheet at its maximum. *Arctic and Alpine Research*, **9**, 21–47.
Teller, J. T., Leverington, D. W., and Mann, J. D., 2002. Freshwater outbursts to the oceans from glacial Lake Aggassiz and their role in climate change during the last deglaciation. *Quaternary Science Reviews*, **21**, 879–888.
Thorliefson, L. H., Wyatt, P. H., and Warman, T. A., 1993. Quaternary stratigraphy of the severn and winisk drainage basins, Northern Ontario. *Geological Survey of Canada*, **Bulletin 442**, 59.

Cross-references

Deglaciation
Ice Age
Sea-Level

LAYERING OF SNOW

Rajesh Kumar
School of Engineering and Technology, Sharda University, Greater Noida, NCR, India

Snow layers are formed as a tabular body of snow with younger at top and oldest at the bottom having well defined boundaries of their precipations if at certain gaps (AGI, 1960). The layers are differentiated from the surrounding one due to unique deposition and post-deposition processes. Each layer of snow forms a snow packs which differs in physical and microstructural properties from those above and below. The layering sequence and its characteristics govern thermal, physical, and mechanical properties of the snow pack. The strength of the snow pack and the transport of air, water, and heat through it are also dependent on layer's characteristics. Under natural conditions they exhibit irregular boundaries and a wide range of grain and bond characteristics when traced laterally.

The definition focuses on the fact that the microstructure (grain size, shape, and arrangement and nature of bonds) differs from one layer to another. Though the layering seems simple, the real snow layers can be complex (Matthew and Carl, 2004). The knowledge about snow mechanics is very crucial in dealing with the snow avalanche formation and hazard mitigation measures. Snow stability depends on the layering of snow. The most relevant mechanical properties like compressive, tensile, and shear strength of the individual snow layers within the snow cover vary significantly in space and time. Local observations of snow layers are used as the basis for spatial extrapolation of snow properties and for establishing a time record of snow deposition.

Bibliography

AGI (American Geological Institute), 1960. *Dictionary of Geologic Terms*. Garden City, NY: Anchor Books, 472 pp.
Matthew, S., and Carl, B., 2004. Scales of spatial heterogeneity for perennial and seasonal snow layers. *Annals of Glaciology*, **38**, 253–260.

LIDAR IN GLACIOLOGY

Michael N. Demuth
Glaciology Section, Geological Survey of Canada, Earth Sciences Sector Program on Climate Change Geoscience, Natural Resources Canada, Ottawa, ON, Canada

Synonyms

Laser altimetry; Laser radar (considered misleading); Laser swath mapping as used in *Airborne Laser Swath Mapping* (ALSM); Laser terrain mapping as used in *Airborne Laser Terrain Mapping* (ALTM)

Definition

LiDAR. Coined from "**L**ight **D**etection **A**nd **R**anging"
Glaciology. The study of glaciers
LASER. Coined from "**L**ight **A**mplification by **S**timulated **E**mission of **R**adiation"

Introduction

The study of the Earth's glaciers and ice sheets is of tremendous importance as their fluctuation has consequences on sea level, river flow, ecosystem functioning, ocean circulation, and climate stability. Recent studies have shown that the Earth's small glaciers are in measurable decline on account of secular atmospheric warming (Kaser et al., 2006; UNEP/WGMS, 2009), and whose environmental services (e.g., hydrological regulation) vary regionally – from short-term flow augmentation to long-term decline (Bonardi, 2008; Casassa et al., 2008; Sauchyn et al., 2008). There is considerable concern regarding the state and evolution of the Earth's larger glacier systems and the ice sheets, and their effect on global sea levels (Abdalati et al., 2002; Arendt et al., 2004; Zwally et al., 2002b; Rignot and Thomas, 2002; Thomas et al., 2006; Bamber et al., 2007; van de Wal et al., 2008; Alley et al., 2009; Thomas et al., 2009; Vinther et al., 2009).

Increasingly, remote sensing tools have been used to study and understand in a more comprehensive, regional manner, the sign, magnitude, rate, and causality of the Earth's glacier and ice sheet mass balance changes. Reflecting on the Greenland ice sheet, Reeh (1999) suggested that modern observation methods in combination with trimline observations, large-scale snow accumulation and mass flux estimates, and ice sheet modeling could reduce the uncertainty associated with understanding its mass balance variation. It has also been recognized for some time that the worldwide glacier surveillance strategy has historically been biased to relatively small glacier sizes, with large glacier systems being relatively underrepresented (Haeberli et al., 1998). The application of laser-based detection and ranging strategies, including the support they provide for glacier and ice sheet mass and energy balance studies, plays a key role in addressing

these thematic concerns, methodological opportunities, and surveillance biases.

The following reviews the principle of lidar, its integration as an instrument in typical glacier surveillance applications, and important error considerations. The capability of lidar is illustrated with numerous examples from the available literature. Survey planning considerations and specific technical challenges are also discussed.

Lidar ranging/swath mapping principles

Lidar for range finding has been in use since the 1970s (e.g., Measures, 1984), and provides long-distance ranging capability to ascertain the position of planetary satellites and moons as applied to geodesy and related fields. This entry concerns laser ranging and detection of the surface of the Earth's glaciers and ice sheets from fixed points, aircraft or artificial satellites, with an emphasis on swath mapping from aircraft.

Lidar-operating principles are generally similar to those of microwave-based RaDAR (**Ra**dio **D**etection **A**nd **R**anging) systems, but instead make use of "light." This light is commonly in the form of near-infrared radiation pulses emitted by a laser. This laser energy interacts with surface features and upon scattering may then return back to a coincident detector, enabling "time of flight" (t) measurement. The range is simply:

$$r = c\frac{t}{2} \tag{1}$$

where c is the velocity of light.

In a typical scanning or swath mapping configuration, laser pulses are directed toward the Earth's surface by employing an oscillating or nutating mirror. This results in a scanning pattern of measurements. In an airborne deployment, this pattern repeats itself along-track. The ground measurement locations are in fact of finite size, and so the matter of laser beam divergence determines the effective illuminated footprint dimensions over which the detection and ranging occurs. Terrain orientation and target range are chief factors, with the spatial coherence of the light over the target surface being a function of the quality of the laser light and the influence of the atmosphere between the source and the target. While usually described as some fraction of a probability density function, aspects of the positional probability and the terrain orientation can complicate defining the footprint dimension.

A key element in a lidar-based topographic mapping system is locating the reference axes of the lidar boresite/detector relative to a spatial reference system for the Earth. For an airborne application, for example, this is enabled by continuously measuring the attitude (pitch, roll, yaw) and position of the aircraft (Figure 1). The former is generally determined with an "inertial measurement unit" (IMU) or outputs from a suitably equipped "inertial navigation system" (INS), while the later is derived from measurements obtained with the aid of Global Navigation Satellite Systems (GNSS; e.g., GPS and/or, GLONASS). Simultaneous GNSS data is collected over a known ground control point within the survey baseline to enable differential correction of the platform position data. "Mechanical offset" measurements between the reference axes, the IMU sensor and the GNSS receiver antenna phase center must also be made (Figure 1). In some systems, the entire laser sensor head is stabilized with gimbals, while other systems use attitude and position data to feedback to and control the scanner mirror directly so that the generated swath remains stable regardless of changes in the aircraft orientation.

Software is used to extract ground-point positions relative to the spatial reference system. The platform velocity, scanner rate, laser pulse repetition frequency (PRF), and IMU data rate for most airborne applications will also require the use of software to project the position of the measurement platform between those determined with the low data rate GNSS measurements (typically 1–2 Hz).

Typical laser scanning systems may employ "first-pulse" and "last-pulse" measurement modes, where the former measures the range between the initial outgoing pulse and the first return pulse detected, while the latter measures the range between the initial outgoing pulse and the last return pulse detected. This may prove useful for "surfaces" having a complex vertical structure. In many systems, the power of the laser return pulse is recorded in the form of an intensity measurement, usually expressed as a function of the percent reflectance of the measured surface. This data can be used to assess the quality of the range measurements as well as give an indication of surface properties.

In the case of a lidar mounted onboard an artificial satellite (e.g., the Global Laser Altimeter System, GLAS, aboard the NASA/EOS Ice Cloud and Elevation Satellite, ICESat; Zwally et al., 2002a), precision orbit determination, timing and geo-location are enabled with GNSS measurements, while "star trackers" are utilized to effect platform pointing and stability control.

A comprehensive treatment of lidar ranging practice can be found in Wehr and Lohr (1999).

Error considerations

Critical to assessing the total survey error budget and the uncertainty associated with, for example, a digital elevation model (DEM) are two major sources of error in lidar data: (1) the forward propagation of individual system component errors and (2) the backward propagation of external contributions such as those manifested by terrain slope.

Starting with Favey et al. (1999) there began a number of efforts where error considerations were discussed with increasing thoroughness (e.g., Krabill et al., 2002;

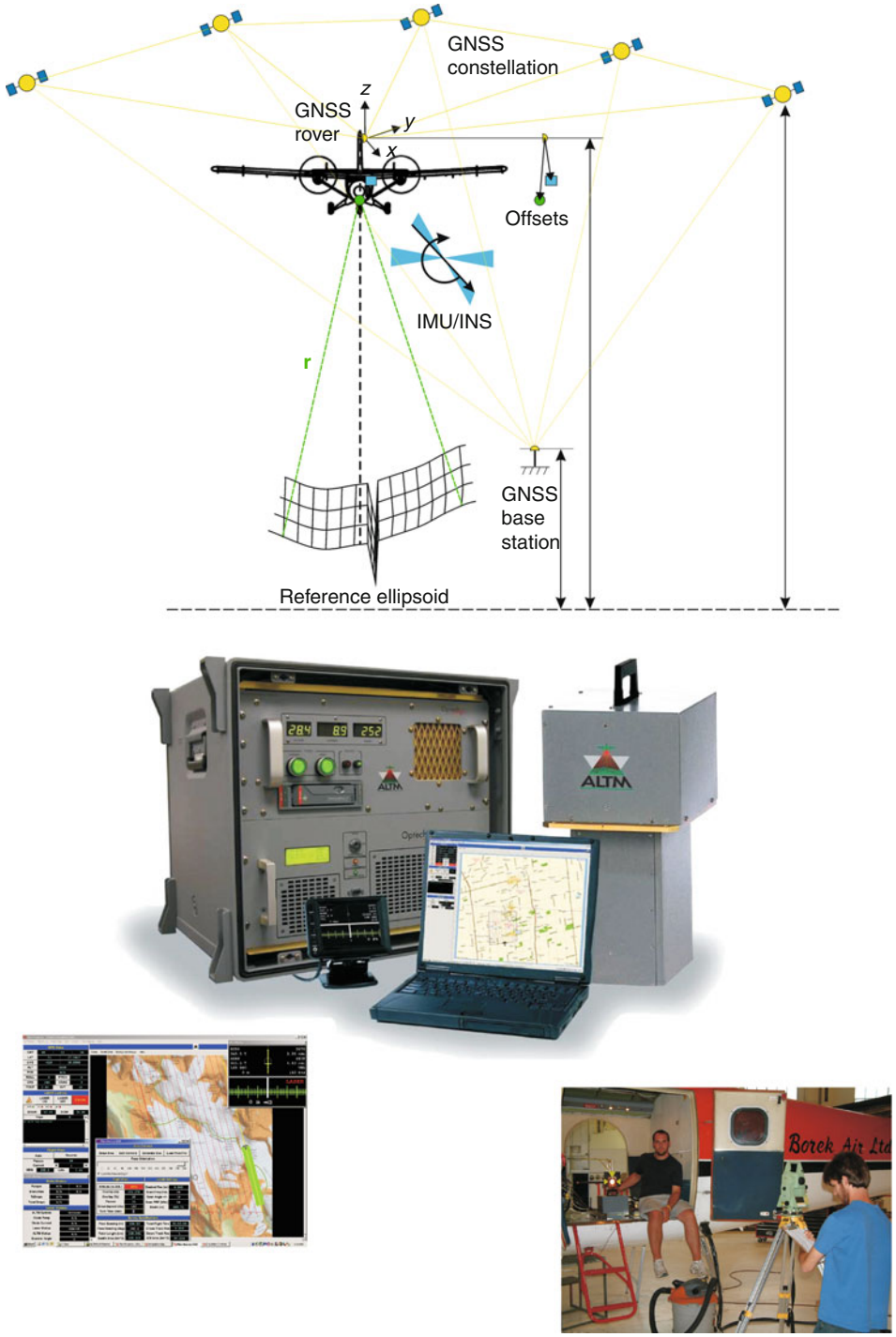

LIDAR in Glaciology, Figure 1 *Top*: Schematic of the measurement and reference framework for airborne lidar mapping; *Middle*: Typical ALTM system components including, clockwise from *top left*: console containing the control module, data storage, IMU and GNSS system interface and laser power supply; laser/mirror assembly; notebook computer/operator interface; pilot display; *Bottom*: Surveying mechanical offsets for an installation in a de Havilland Canada Twin Otter (System photograph courtesy Optech Inc., Toronto Canada; photograph of mechanical offset measurement courtesy Chris Hopkinson and the Canadian Consortium for Lidar Environmental Applications Research, C-CLEAR).

Lutz et al., 2003; Hodgson and Bresnahan, 2004). This was in response to the problems associated with steep terrain, detecting small changes over large areas, GNSS ambiguity resolution, and long survey baselines. Work in other fields (e.g., Davenport et al., 2004) has benefited error assessment considerations for glaciological applications, particularly as it concerns to high point-density and surface morphology studies. Goulden (2009) provides a comprehensive treatment of terrain slope errors in which initial errors are first estimated by propagating the error of the individual measurement systems in the LiDAR system using the General Law of Propagation of Variances. These are then cast in terms of the effect of the local slope to produce a "worst-case scenario" of the actual terrain. For a variety of heights above ground level (AGL) and scan angles, Goulden and Hopkinson (2010) provide a thorough treatment of forward error propagation as it concerns the laser beam divergence, and IMU and GNSS subsystems specifically.

Vibration modes having their origin in the measurement platform can also impart errors through the nature of gimbal or scanner mechanical structures, though most of these problems can be ameliorated through control system design and structural tuning. For installations on aircraft where the location of various system components may be dictated by cable routing, power supplies, structural bulkheads, and aperture and antenna locations, aeroelastic resonance may impart particularly troublesome consequences on the final data. These can include the manifestation of surface roughness where there is none, or noise that precludes the study of surface roughness (personal communication, Robert Gurney).

A better understanding of the error budgets associated with the application of lidar has manifested the broader utility of lidar as a tool in glaciology, including determining survey expectations a priori, assessing specifications provided by commercial lidar manufacturers, establishing lidar data acquisition/mission planning standards, and the development of some novel applications.

Lidar in practice

Almost all field glaciologists, young and not so young, will be familiar with laser range finding as part of simple trigonometric "theodolite" surveys or with "total station" instruments. Range measurements are made by discrete, manual repositioning of a reflector prism, though there are motorized total station systems that can follow the reflector prism continuously. Techniques employing GNSS have largely replaced this method of topographic mapping.

More recently, ground-based scanning lidar has been used to automatically map surfaces with sub-centimeter range and positional accuracy over ranges spanning several meters to more than 1 km (e.g., Intelligent Laser Ranging and Imaging System or ILRIS; www.optech.ca). Typical deployments involve locating the system over several established ground control points, with the resulting scanner data ingested by software to produce 3-D models of exceptional quality. ILRIS and similar systems are used primarily for engineering applications requiring high tolerances, but have also seen use in periglacial geomorphology studies. Because engineering applications dominate the commercial ILRIS market, and therefore must operate as "eye-safe" (e.g., urban environments), 1,550 ηm laser light is employed. For snow and ice, particularly in the presence of any melting, 1,550 ηm is considered unsuitable; because both transmission and specular reflection occur, laser return dropout rates are extremely high (personal communication, Chris Hopkinson). As such, they have not seen much use in the glaciological community. Nevertheless, the author is aware of one proof-of-concept effort that included a quantitative assessment of the range capability of an ILRIS instrument over glacier ice and snow-covered surfaces (Hopkinson, 2004).

Airborne lidar applications are now common despite the high instrument and software costs associated with commercially available systems, and the high aviation costs associated with typical surveys. Garvin (1997) reviewed the contemporary efforts of the 1990s, including the preeminent work of Krabill et al. (1995) who measured surface elevation change over the Greenland ice sheet and its outlet glaciers using the NASA Wallops Flight Facility, Airborne Topographic Mapper (ATM). This and subsequent missions have contributed to much of the Greenland ice sheet literature quoted in the introduction (Figure 2). In 1995, NASA's ATM team collaborated with the Glaciology Group of the Geological Survey of Canada (GSC) to begin repeat altimetry measurements over all of the major ice caps of the Canadian Arctic Islands (Abdalati et al., 2004), a collaborative effort that continues to this day. Echelmeyer et al. (1996) utilized a "pencil" lidar over the extensive glacier systems of Alaska, and in subsequent efforts, expanded the investigation to include the numerous accumulation areas located in the Yukon Territory, Canada that feed some of the Alaskan glaciers. With this data, Arendt et al. (2002) reported on the significant sea level contributions from this relatively little studied region. Notably, this effort was enabled by assembling a system "off-the-shelf" and installing it in a private light aircraft flown by Echelmeyer.

Smaller-scale efforts to map surface topography were initiated over a single small glacier in Norway by Kennet and Eiken (1997) using an early-generation commercial scanner system. They compared their results to those derived from the application of traditional stereo photogrammetry. Favey et al. (1999) reported on the utility of repeat scanning lidar surveys for estimating volume changes over a small glacier in Switzerland, as did Hopkinson et al. (2001) and Hopkinson and Demuth (2006) for a large ice field in the Canadian Rocky Mountains and its outlet glaciers (Figure 2).

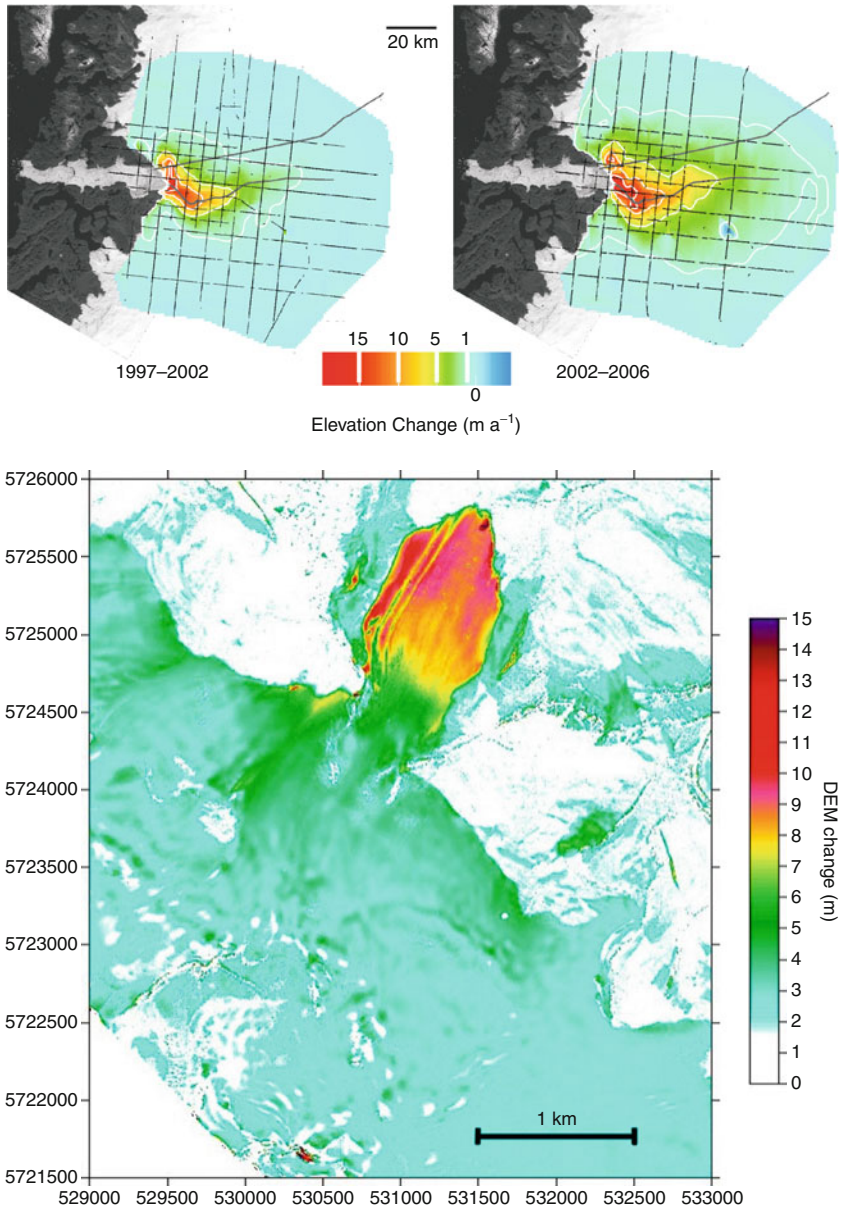

LIDAR in Glaciology, Figure 2 Inferred surface elevation change determined from repeat laser altimetry. *Top*: Jakobshavn Isbræ, Greenland, 1997–2002–2006, to a point where it converges into its rapidly flowing outlet (After Thomas et al., 2009; with permission International Glaciological Society); *Bottom*: Peyto Glacier, Canadian Rocky Mountains, 2000–2002 (After Hopkinson and Demuth, 2006; with permission Canadian Aeronautical and Space Institute).

If surveys are conducted with a high enough point measurement density, mapping surface features such as meltwater channels, moulins, and other thermal or mechanical surface manifestations is possible e.g., (Figure 3; see also Hopkinson et al., 2001; Arnold et al., 2006). Repeat surface mapping can enable surface feature tracking in support of glacier motion studies (Abdalati and Krabill, 1999; Arnold et al., 2006; Hopkinson and Demuth, 2006; Hopkinson et al., 2009). Several investigators have utilized return pulse intensity values to map the distribution of seasonal snow, firn, and ice over the glacier surface e.g., (Figure 4; see also Lutz et al., 2003; Arnold et al., 2006; Hopkinson and Demuth, 2006).

Airborne lidar has enabled detailed investigations in regions that are, for the most part, very difficult to access due to weather and terrain. These "hurry up and wait"

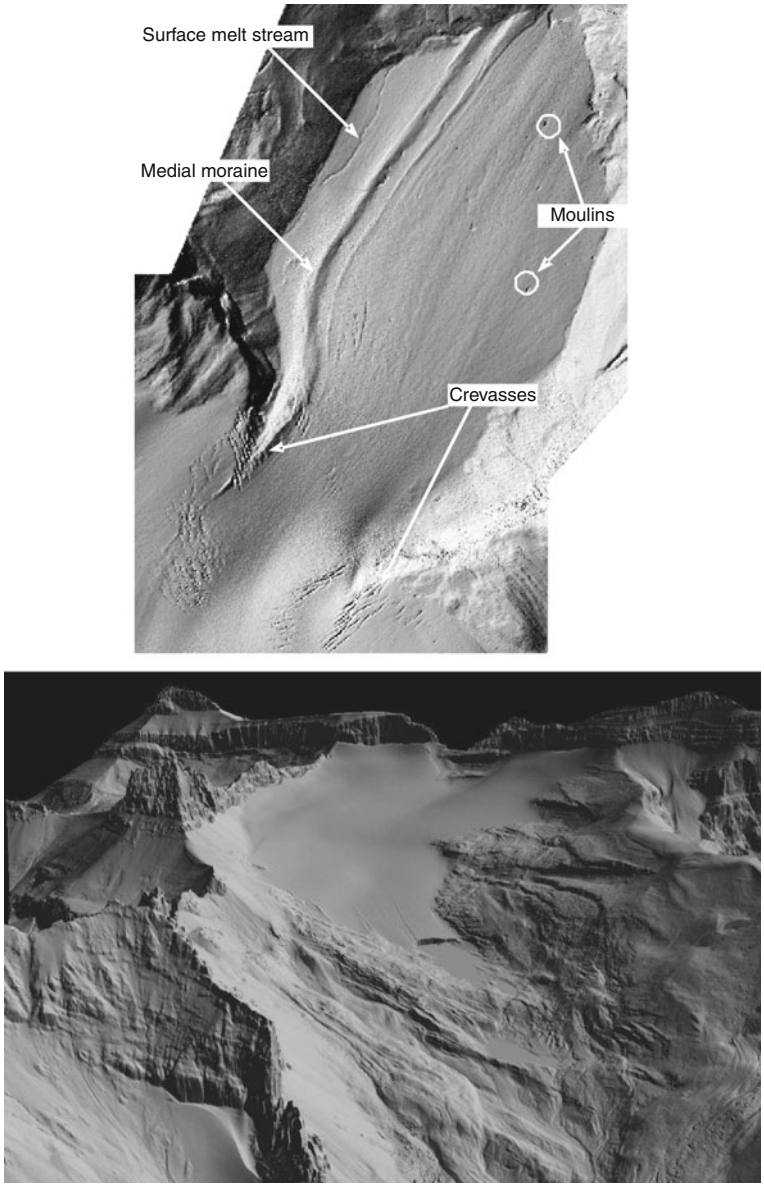

LIDAR in Glaciology, Figure 3 *Top*: Shaded-relief rendering of last-pulse data (gridded at 2 m resolution) collected over the terminus of Peyto Glacier, Canadian Rocky Mountains, 2002. Crevasses, meltwater streams, moulins and medial moraine forms are clearly evident. *Bottom*: Oblique rendering of the Ram River Glacier and the upper Ram River Valley, Canadian Rocky Mountains, 2002. The glacier has retreated out of an over deepened basin resulting, in this instance, in a calving terminus. Surface meltwater streams are also evident. (Data courtesy of C-CLEAR, Optech Inc. and the Geological Survey of Canada).

scenarios, where taking advantage of brief periods of fair weather is key, include studies of glacier elevation change in Patagonia (Keller et al., 2007), and assessing the mechanism and volumes of material involved in ice and rock avalanche events in the Icefield Ranges of Canada's Saint Elias Mountains (Lipovsky et al., 2008).

High-resolution ALTM has also been used in support of glacier energy-balance modeling and hydrology (Chasmer and Hopkinson, 2001; Arnold and Rees, 2003; Hopkinson and Demuth, 2006; Hopkinson et al., 2010). Lidar-derived DEMs can support satellite-based glaciological studies including the terrain-correction of SAR imagery (e.g., Wivell et al., 1992), and removing the topography effect necessary in the application of InSAR for glacier motion studies. Satellite altimetry cal/val campaigns routinely utilize lidar. For example, the CryoSat-2 (e.g., Wingham et al., 2006) calibration/validation effort will utilize ICESat low-slope crossovers, and under-flights with the NASA ATM. Lidar has also been used in the validation of glacier DEMs derived from the Shuttle Radar (SRTM)

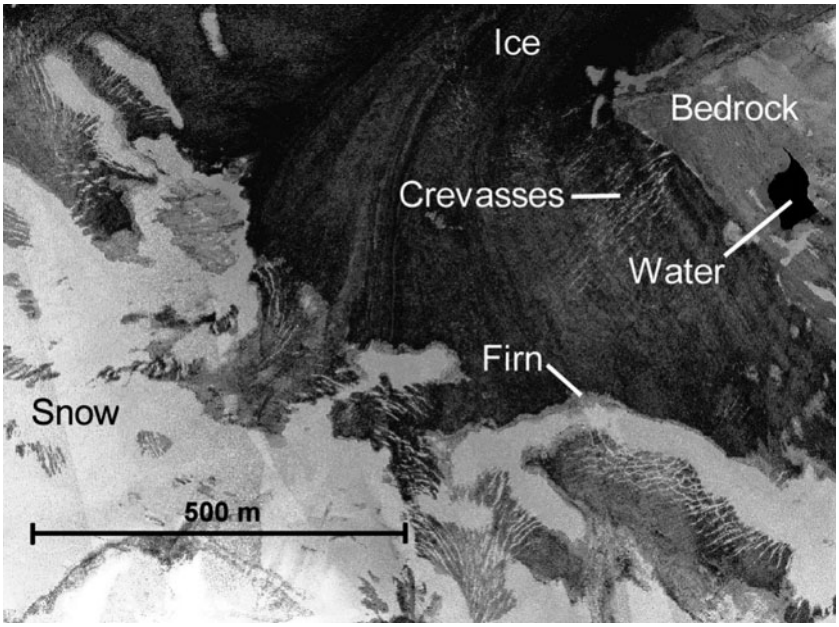

LIDAR in Glaciology, Figure 4 Return pulse intensity image from a portion of Peyto Glacier near its equilibrium line, demarcating regions of snow, firn, and ice. (After Hopkinson and Demuth, 2006; by permission Canadian Aeronautical and Space Institute).

and the Advanced Spaceborne Thermal Emission Radiometer (ASTER) instrument aboard NASA's EOS/Terra spacecraft.

Lidar-based altimetry from artificial satellites is currently the realm of ICESat's GLAS instrument (Zwally et al., 2002a), which has seen service over both ice sheet interiors, their margins and ice streams, ice shelves, and the large glacier systems of Alaska and Svalbard (e.g., Csatho et al., 2005; and overview by Zwalley, 2005).

Mission planning

Returning again to airborne swath mapping, a few salient points related to mission planning are now provided.

Survey goals and aviation resources will, to a large degree, dictate the ground-point measurement density, which is in turn realized by adjusting survey system parameters: laser PRF, scanner angle/field of view, scanner rate; and flight variables: height AGL and ground speed. Estimating the nominal point-spacing will also vary according to the type of scanner/mirror configuration employed. High point-densities may be desirable for glacier morphological and surface facies studies, whereas, lower point-densities may be acceptable for DEM generation so long as topographic noise does not confound the survey goals. It should also be noted that due to the finite speed of light, the laser PRF will be height limited; and that "eye-safe" laser range may impose minimum flying heights in regions where, for example, recreational alpine ski touring is popular.

Notwithstanding aviation and meteorological considerations, mission planning for swath mapping typically involves determining the number of flight lines (fl) for a given width ($\overleftrightarrow{Y}$) of the planned survey area (perpendicular to the flightline direction), and the desired swath overlap fraction (olp):

$$fl = \frac{\overleftrightarrow{Y}}{sw(1 - olp)} \tag{2}$$

where sw is the swath width given by:

$$sw = 2h \tan\left[\frac{\theta_{sc}}{2}\right] \tag{3}$$

and where h is the height above ground and θ_{sc} is the scanner angle/field of view. Overlap is desirable for error checking and stitching swath data for contiguous mapping.

"Terrain following" is often employed to maintain a nominal height AGL, resulting in a more uniform swath and overlap widths and generally results in fewer laser return dropouts. Aviation considerations include flying the aircraft within gimbal and IMU tolerances and making rudder turns that prevent the loss of signal lock with the GNSS.

Challenges

Several additional technical challenges confront the user of lidar-derived terrain information, particularly as it concerns the detection and interpretation of height change data. In many glaciological applications, we are concerned with detecting small changes over large areas. Notwithstanding what has already been discussed with respect to coupled system and terrain errors, attention must be paid to the vertical reference systems used in precision height

measurement. A good overview is provided by Töyrä et al. (2003), albeit confined to the Canadian Spatial Reference System. A more general overview describing the representation of the Earth's surface undulations can be found at: http://www.kartografie.nl/geometrics/Reference%20surfaces/body.htm.

While repeat lidar mapping can lead to relatively straightforward estimates of surface elevation change, deriving surface mass balances over the accumulation area will require additional information describing the contribution to elevation change of snow densification, accumulation, and ice flow/divergence. For example, densification alone can manifest thinning, while in actuality there may have been zero mass change. Conversely, thickening may be the result of changing ice flow conditions – for example, as possibly manifested by a delayed Little Ice Age cooling having stiffened the ice near the glacier bed, therefore retarding the flow of ice (personal communication, Martin Sharp).

While alluded to previously, instrument and aviation costs are likely the largest challenge to the systematic use of lidar in the study of glaciers. To date this has been ameliorated by developing research consortia such as the Canadian-based C-CLEAR, and international cooperation founded by NASA's Wallops Flight Facility and the Geodynamics Department of the Danish National Space Centre. Indeed, these entities have been the means to developing research applications in both Hemispheres. In many jurisdictions, national aviation laboratory facilities cannot be seen to compete with the private sector airborne survey industry, and so valuable surveillance capacity may sit underutilized. C-CLEAR regularly conducts national-scale, multi–theme survey missions where all research stakeholders share the aviation costs. Other groups have endeavored to construct integrated systems by assembling off-the-shelf components and installing them in private light aircraft (Geophysical Institute, University of Alaska Fairbanks) or coordinating installations with air force or navy assets (Centro de Estudios Científicos, Chile).

Despite these challenges, the literature suggests that lidar-based surveys of glacier surface elevation change and other variables will assist differentiating interannual variability from long-term trends – a critical aspect of glaciological study in a water resources and sea level context.

Summary

This entry has presented a brief review of the principle of light detection and ranging, and a description of a variety of laser-based systems used in glaciological studies. A discussion of error considerations has been provided, and the capability of lidar was illustrated with numerous examples from the available literature. Basic survey planning considerations and some of the specific challenges of using lidar in the study of glaciers and ice sheets were discussed. A bibliography for further study and reference accompanies this text.

Bibliography

Abdalati, W., and Krabill, W., 1999. Calculation of ice velocities in the Jakobshavn Isbrae area using airborne laser altimetry. *Remote Sensing of Environment*, **67**, 194–204.

Abdalati, W., Krabill, W., Frederick, E., Manizade, S., Martin, C., Sonntag, J., Swift, R., Thomas, R., Yungel, J., and Koerner, R., 2004. Elevation changes of ice caps in the Canadian Arctic Archipelago. *Journal of Geophysical Research*, **109**, F04007, doi:10.1029/2003JF000045.

Alley, R. B., Andrews, J. T., Clarke, G. K. C., Cuffey, K. M., Funder, S., Marshall, S. J., Mitrovica, J. X., Muhs, D. R., and Otto-Bleisner, B., 2009. Past extent and status of the Greenland ice sheet. In *Past Climate Variability and Change in the Arctic and at High Latitudes*. U.S. Climate Change Program and Subcommittee on Global Change Research. U.S. Geological Survey, Reston, VA, pp. 303.357.

Arendt, A. A., Echelmeyer, K. A., Harrison, W. D., Lingle, C. S., and Valentine, V. B., 2002. Rapid wastage of Alaska glaciers and their contribution to rising sea level. *Science*, **297**, 382.

Arnold, N. S., and Rees, W. G., 2003. Self-similarity in glacier surface characteristics. *Journal of Glaciology*, **49**, 547–554.

Arnold, N. S., Rees, W. G., Devereux, B. J., and Amable, G. S., 2006. Evaluating the potential of high-resolution airborne LiDAR data in glaciology. *International Journal of Remote Sensing*, **27**(6), 1233–1251, doi:10.1080/01431160500353817.

Bamber, J. L., Alley, R. B., and Joughin, I., 2007. Rapid response of modern day ice sheets to external forcing. *Earth and Planetary Science Letters*, **257**, 1–13.

Bonardi, L. (ed.), 2008. Mountain glaciers and climate changes in the last century. *Terra Glacialis*, Special Issue, 239 pp.

Casassa, G., López, P., Pouyaud, B., and Escobar, F., 2008. Detection of changes in glacial run-off in alpine basins: examples from North America, the Alps, central Asia and the Andes. *Hydrological Processes*, **23**(1), 31–41.

Chasmer, L., and Hopkinson, C., 2001. Using airborne LASER altimetry and GIS to assess scale-induced radiation-loading errors in a glacierized basin. In *Proceedings of the 58th Eastern Snow Conference*, May 17–19, 2001, Ottawa, Canada, pp. 195–205.

Csatho, B., Ahn, Y., Yoon, T., van der Veen, C. J., Vogel, S., Hamilton, G., Morse, D., Smith, B., and Spikes, V. B., 2005. ICESat measurements reveal complex pattern of elevation changes on Siple Coast ice streams, Antarctica. *Geophysical Research Letters*, **32**, L23S10, doi:doi:10.1029/2005GL024306.

Davenport, I. J., Holden, N., and Gurney, R. J., 2004. Characterizing errors in airborne laser altimetry data to extract soil roughness. *IEEE Transactions on Geoscience and Remote Sensing*, **42**, 2130–2141.

Echelmeyer, K. A., Harrison, W. D., Larsen, C. F., Sapiano, J., Mitchell, J. E., Demallie, J., Rabus, B., Adalgeirsdottir, G., and Sombardier, L., 1996. Airborne surface profiling of glaciers: a case study in Alaska. *Journal of Glaciology*, **42**, 538–547.

Favey, E., Geiger, A., Gudmundsson, G. H., and Wehr, A., 1999. Evaluating the potential of an airborne laser-scanning system for measuring volume changes of glaciers. *Geografiska Annaler*, **81A**, 555–561.

Garvin, J. B., 1997. *Monitoring glaciers with airborne and spaceborne laser altimetry.* United States Geological Survey Open-file Report, 98-31, Williams Jr., R. S., and Ferrigno J. G. (eds.): URL: http://pubs.usgs.gov/of/1998/of98-031/index.htm.

Goulden, T., 2009. *Prediction of Error Due to Terrain Slope in Lidar Observations*. Unpublished Master of Science in Engineering thesis, Canada, The University of New Brunswick, 144 pp.

Goulden, T., and Hopkinson, C., 2010. The forward propagation of integrated system component errors within airborne lidar

data. *Photogrammetric Engineering and Remote Sensing*, **76**, 589–601.
Haeberli, W., Hoelzle, M., and Suter, S. (eds.), 1998. *Into the Second Century of Worldwide Glacier Monitoring: Prospects and Strategies*. Paris: UNESCO. Studies and Reports in Hydrology, Vol. 56, p. 227.
Hodgson, M., and Bresnahan, P., 2004. Accuracy of airborne LiDAR-derived elevation: empirical assessment and error budget. *Photogrammetric Engineering and Remote Sensing*, **70**, 331–339.
Hopkinson, C., 2004. *Place Glacier Terrain Modeling and 3D Laser Imaging*. Contract Report No. TSD051603X. Prepared for the National Glaciology Program of the Geological Survey of Canada, M.N. Demuth, Scientific Authority, 22 pp + digital files on CD.
Hopkinson, C., Chasmer, L., Munro, D. S., and Demuth, M. N., 2010. The influence of DEM resolution on simulated solar radiation-induced glacier melt. *Hydrological Processes*, **24**(6), 775–788.
Hopkinson, C., and Demuth, M. N., 2006. Using airborne lidar to assess the influence of glacier downwasting on water resources in the Canadian Rocky Mountains. *Canadian Journal of Remote Sensing*, **32**(2), 212–222.
Hopkinson, C., Demuth, M., Sitar, M., and Chasmer, L., 2001. Applications of lidar mapping in a glacierised mountainous terrain. In Stein, T. I. (ed.), *IGARSS'01: Proceedings of the International Geoscience and Remote Sensing Symposium*, July 9–14, Sydney, Australia. CDROM. IEEE, New York.
Hopkinson, C., Demuth, M. N., Barlow, J., Sitar, M., Young, G., Pomeroy, J., and Munro, D. S., 2009. Investigating glacier dynamics using temporal air photo, LiDAR and oblique thermal imagery at Peyto Glacier; an overview. In *Proceedings of the Canadian Symposium on Remote Sensing*, June 22–25, Lethbridge, Alberta. Canadian Aeronautical and Space Institute.
Kaser, G., Cogley, J. G., Dyurgerov, M. B., Meier, M. F., and Ohmura, A., 2006. Mass balance of glaciers and ice caps: consensus estimates for 1961-2004. *Geophysical Research Letters*, **33**, L19501, doi:10.1029/2006GL027511.
Keller, K., Casassa, G., Rivera, A., Forsberg, R., and Gundestrup, N., 2007. Airborne laser altimetry survey of Glacier Tyndall, Patagonia. *Global and Planetary Change*, **59**, 101–109, doi:10.1016/j.gloplacha.2006.11.039 DOI:dx.doi.org.
Kennet, M., and Eiken, T., 1997. Airborne measurement of glacier surface elevation by scanning laser altimeter. *Annals of Glaciology*, **24**, 235–238.
Krabill, W. B., Thomas, R., Jezek, K., Kuivinen, K., and Manizade, S., 1995. Greenland ice sheet thickness changes measured by laser altimetry. *Geophysical Research Letters*, **22**, 2341–2344.
Krabill, W. B., Abdalati, W., Frederick, E. B., Manizade, S. S., Martin, C. F., Sonntag, J. G., Swift, R. N., Thomas, R. H., and Yungel, J. G., 2002. Aircraft laser altimetry of elevation changes of the Greenland ice sheet: technique and accuracy assessment. *Journal of Geodynamics*, **34**, 357–376.
Lipovsky, P. S., Evans, S. G., Clague, J. J., Hopkinson, C., Couture, R., Bobrowsky, P., Ekström, G., Demuth, M. N., Delaney, K. B., Roberts, N. J., Clarke, G. K. C., and Schaeffer, A., 2008. The July 2007 rock and ice avalanches at Mount Steele, St. Elias Mountains, Yukon, Canada. *Landslides*, doi:10.1007/s10346-008-0133-4.
Lutz, E., Geist, T., and Stotter, J., 2003. Investigations of airborne laser scanning signal intensity on glacial surfaces – utilizing comprehensive laser geometry modelling and orthophoto surface modelling (a case study: Svartisheibreen, Norway). In Mass, H.-G., Vosselman, G., and Streilein, A. (eds.), *Proceedings of the ISPRS Workshop on 3D Reconstruction from Airborne Laser Scanner and InSAR Data*, October 8–10, Dresden, Germany, pp. 101–106.
Measures, R. M., 1984. *Laser Remote Sensing*. New York: Wiley.
Reeh, N., 1999. Mass balance of the Greenland ice sheet: can modern observation methods reduce the uncertainty? *Geografiska Annaler*, **81A**, 735–742.
Rignot, E., and Thomas, R. H., 2002. Mass balance of Polar ice sheets. *Science*, **297**, 1502–1506.
Sauchyn, D., Demuth, M. N., and Pietronrio, A., 2008. Upland watershed management and global change: Canada's Rocky Mountains and western plains. In Garrido, A., and Dinar, A. (eds.), *Managing Water Resources in a Time of Global Change: Mountains, Valleys and Floodplains*, Contributions from the Rosenberg International Forum on Water Policy, Vaux Jr. H. (series ed.). London: Routledge, pp. 49–66.
Thomas, R., Frederick, E., Krabill, W., Manizade, S., and Martin, C., 2006. Progressive increase in ice loss from Greenland. *Geophysical Research Letters*, **33**, L10503, doi:10.1029/2006GL026075.
Thomas, R., Frederick, E., Krabill, W., Manizade, S., and Martin, C., 2009. Recent changes on Greenland outlet glaciers. *Journal of Glaciology*, **55**(189), 147–162.
Töyrä, J., Pietroniro, A., Hopkinson, C., and Kalbfleisch, W., 2003. Assessment of airborne scanning laser altimetry (lidar) in a deltaic wetland environment. *Canadian Journal of Remote Sensing*, **29**(6), 718–728.
UNEP/WGMS, 2009. Global Glacier Changes – Facts and Figures: www.grid.unep.ch/glaciers/.
van de Wal, R. S. W., Boot, W., van den Broeke, M. R., Smeets, C. J. P. P., Reijmer, C. H., Donker, J. J. A., and Oerlemans, J., 2008. Large and rapid melt-induced velocity changes in the Ablation Zone of the Greenland Ice Sheet. *Science*, **321**, 111–113.
Vinther, B. M., Buchardt, S. L., Clausen, H. B., Dahl-Jensen, D., Johnsen, S. J., Fisher, D. A., Koerner, R. M., Raynaud, D., Lipenkov, V., Andersen, K. K., Blunier, T., Rasmussen, S. O., Steffensen, J. P., and Svensson, A. M., 2009. Holocene thinning of the Greenland ice sheet. *Nature*, **461**, 385–388, doi:10.1038/nature08355.
Wehr, A., and Lohr, U., 1999. Airborne laser scanning — an introduction and overview. *ISPRS Journal of Photogrammetry and Remote Sensing*, **54**, 68–82.
Wingham, D. J., Francis, C. R., Baker, S., Bouzinac, C., Brockley, D., Cullen, R., de Chateau-Thierry, P., Laxon, S. W., Mallow, U., Mavrocordatos, C., Phalippou, L., Ratier, G., Rey, L., Rostan, F., Viau, P., and Wallis, D. W., 2006. CryoSat: A mission to determine the fluctuations in Earth's land and marine ice fields. *Advances in Space Research*, **37**, 841–871.
Wivell, C. E., Steinwand, D. R., Kelly, G. G., and Meyer, D. J., 1992. Evaluation of terrain models for the geocoding and terrain correction of synthetic aperture radar (SAR) images. *IEEE Transactions on Geoscience and Remote Sensing*, **30**(6), 1137–1144.
Zwalley, H. J., 2005. Overview of scientific advances from the ICESat mission. *EOS Transactions, American Geophysical Union*, **86**(52), Fall Meeting Supplement, Abstract C33A-01.
Zwally, H. J., Schutz, B., Abdulati, W., Abshire, J., Bentley, C., Brenner, A., Bufton, J., Dezio, J., Handcock, D., Harding, D., Herring, T., Minster, B., Quinn, K., Palm, S., Spinhirne, J., and Thomas, R., 2002a. ICESat's laser measurements of polar ice, atmosphere, ocean and land. *Journal of Geodynamics*, **34**, 405–445.
Zwally, H. J., Abdalati, W., Herring, T., Larson, K., Saba, J., and Steffen, K., 2002b. Surface melt-induced acceleration of Greenland ice-sheet flow. *Science*, **297**, 218–222.

Cross-references

Automated Glacier Mapping
Digital Elevation Model Generation Over Glacierized Region

Equilibrium-Line Altitude (ELA)
Glacier Mass Balance
Glacier Motion/Ice Velocity
Glaciology
GPS in Glaciology, Applications
Ice Sheet Mass Balance
ICESat Data in Glaciological Studies
Optical Remote Sensing of Alpine Glaciers
Synthetic Aperture Radar (SAR) Interferometry for Glacier Movement Studies

LITTLE ICE AGE

Rajesh Kumar
School of Engineering and Technology, Sharda University, Greater Noida, NCR, India

There is no agreed beginning year to the Little Ice Age when the world experienced relatively cooler temperatures compared to the present, but it is conventionally defined as a period extending from the sixteenth to the nineteenth centuries when there was expansion of mountain glaciers (http://www.meteo.psu.edu/~mann/shared/articles/littleiceage.pdf; Lamb, 1972; http://earthobservatory.nasa.gov/Glossary/?mode=alpha&seg=l&segend=n). During this period, glaciers in many parts of the world expanded and came down to the lower altitude. It is speculated that the amount of solar radiation emitted by the Sun was low at that time as a periodical phenomenon. Volcanic eruption is accounted for an unexpected blockage of sunlight, leading to worldwide cooling.

Bibliography

http://www.meteo.psu.edu/~mann/shared/articles/littleiceage.pdf
http://earthobservatory.nasa.gov/Glossary/?mode=alpha&seg=l&segend=n
Lamb, H. H., 1972. *The cold Little Ice Age climate of about* 1550 to 1800. *Climate: present, past and future*. London: Methuen, p. 107, ISBN 0-416-11530-6. (noted in Grove 2004:4).

LOBE

Rajesh Kumar
School of Engineering and Technology, Sharda University, Greater Noida, NCR, India

A rounded projection of glacier is known as lobe. Ice lobes are dynamic features within large ice sheets that reflect glacier accumulation and ablation, ice temperature, bedrock topography, ice topography, marginal seas, and ice flow. The ice lobes are the more active parts of the uniform ice sheet. They represent parts that had bordered on each other in different directions or on more passive portions of the ice (Punkari, 1980). Marginal extension of ice stream along broad bedrock trough or valley may be hundreds of kilometers long often terminating in large ice lobes. With the increasing water pressure near the bed of ice lobe, the area of an ice lobe increases while its thickness decreases (Hughes, 1981). The ice is thickest near the central lines of lobe and thinnest near the marginal zone that gives rise to a fan-shaped directions of glacial flow (Reeh, 1982). At the ice margins, thrust moraines and hummocky stagnation topography are more common than single-crested, simple moraines if the ice lobes had repeated advances. Normally terminal moraines are formed at the farthest extent of ice lobe. In the boundary zones of the different ice lobes, there occur exceptionally large glaciofluvial forms and moraines.

Bibliography

http://cgrg.geog.uvic.ca/abstracts/JenningsTerrestrialThe.html.
Hughes, T. J., 1981. Numerical reconstructions of paleo-ice sheets. In The Last Great Ice Sheets, eds *G. H. Denton and T. J. Hughes*, pp. 222–274. John Wiley, New York.
Punkari, M., 1980. The ice lobes of the Scandinavian ice sheet during the deglaciation in Finland. *Boreas*, **9**, 307–310.
Reeh, N., 1982. A Plasticity theory approach to the steady-state shape of a three-dimensional ice sheet. *Journal of Glaciology*, **28**, 431–455.